

ABSTRACT

MISSELL, CHRISTINE ANN. Thermoregulatory adaptations of *Acrocanthosaurus atokensis* – evidence from oxygen isotopes. (Under the direction of Reese Barrick.)

Isotopic analyses of bone phosphate oxygen from a modern alligator, ostrich, and elephant have provided a means for examining diagenesis and thermoregulatory strategy within the dinosaur *Acrocanthosaurus atokensis*. The *Acrocanthosaurus* specimen is assumed to retain an original isotopic signature, based on a lack of linear correlation between $\delta^{18}\text{O}_{\text{phosphate}}$ and structural $\delta^{18}\text{O}_{\text{carbonate}}$, equal standard deviations between $\delta^{18}\text{O}_{\text{phosphate}}$ values for spongy and compact bone, and a significant difference between $\delta^{18}\text{O}_{\text{phosphate}}$ and cement $\delta^{18}\text{O}_{\text{carbonate}}$. Interbone and intrabone temperature variation patterns suggest that *Acrocanthosaurus* followed a homeothermic pattern of heat distribution (i.e. maintenance of a 4°C temperature range). Comparison with the modern animals yields a closer resemblance to the ostrich and elephant versus the alligator, thereby suggesting *Acrocanthosaurus* was endothermic. The *Acrocanthosaurus* sacral spines and palatal bones show evidence of use as heat shedding structures and the braincase yields a significantly higher calculated temperature than the body.

THERMOREGULATORY ADAPTATIONS OF *ACROCANTHOSAURUS*
ATOKENSIS – EVIDENCE FROM OXYGEN ISOTOPES

By
CHRISTINE ANN MISSELL

A thesis submitted to the Graduate Faculty of
North Carolina State University
in partial fulfillment of the
requirements for the Degree of
Master of Science

MARINE, EARTH, AND ATMOSPHERIC SCIENCES

Raleigh

2004

APPROVED BY:

Chair of Advisory Committee

DEDICATION

I would like to dedicate this work to my mother for teaching me the true meaning of strength, perseverance, patience, and good spelling.

BIOGRAPHY

Christine Missell was born and raised in Rochester, NY. She attended the University of Maryland at College Park and graduated in May 2001 with a Bachelors in Geology. After a summer as a teaching assistant for a field camp in Wyoming, she returned to the east coast, moved even further south, and started her Masters at North Carolina State University. Upon completion of her Masters, she returned to Maryland to pursue her PhD in vertebrate paleontology at the University of Maryland. When she isn't partaking in academia, she can be found studying martial arts, rock climbing, enjoying the winter season, or practicing the piano.

ACKNOWLEDGEMENTS

I would like to acknowledge Dr. Reese Barrick, Dr. Dale Russell, Dr. Harold Heatwole, and Dr. Jonathan Karr for their guidance, advice, and helpful comments; Dr. Betsy Bennett, Vince Schneider, and the North Carolina State Museum of Natural History for their assistance with this project; and William Straight and Alan Coulson for their guidance in the lab.

TABLE OF CONTENTS

	Page
LIST OF FIGURES	vi
INTRODUCTION	1
Terminology	1
Previous Research	4
Objectives	9
CHAPTER 1 – EXAMINATION OF MODERN ANIMALS	12
Materials and Methods	12
Phosphate oxygen isotopes	13
Carbonate oxygen and carbon isotopes	14
Standards	15
Results and Discussion	17
Implications to fossil diagenesis	17
Examination of thermoregulation	19
Conclusions	26
Future Work	28
Figures	29
CHAPTER 2 – EXAMINATION OF <i>ACROCANTHOSAURUS ATOKENSIS</i>	45
Materials and Methods	45
Phosphate oxygen isotopes	45
Carbonate oxygen and carbon isotopes	47
Standards	48
Results and Discussion	49
Diagenesis	49
Examination of thermoregulation	52
Conclusions	59
Future Work	60
Figures	61
LIST OF REFERENCES	69
APPENDIX I – Data Tables	76

LIST OF FIGURES

Page

Fig. 1.1 – Ostrich $\delta^{18}\text{O}_{\text{phosphate}}$ vs. $\delta^{18}\text{O}_{\text{carbonate}}$	29
Fig. 1.2 – Elephant $\delta^{18}\text{O}_{\text{phosphate}}$ vs. $\delta^{18}\text{O}_{\text{carbonate}}$	30
Fig. 1.3 – Alligator $\delta^{18}\text{O}_{\text{phosphate}}$ vs. $\delta^{18}\text{O}_{\text{carbonate}}$	31
Fig. 1.4 – Modern animals standard deviation by bone type	32
Fig. 1.5 – Alligator $\delta^{18}\text{O}_{\text{phosphate}}$ per bone	33
Fig. 1.6 – Alligator intrabone temperature variation	34
Fig. 1.7 – Alligator interbone temperature variation	35
Fig. 1.8 – Alligator interbone temperature variation from core body	36
Fig. 1.9 – Elephant $\delta^{18}\text{O}_{\text{phosphate}}$ per bone	37
Fig. 1.10 – Elephant intrabone temperature variation	38
Fig. 1.11 – Elephant interbone temperature variation	39
Fig. 1.12 – Elephant interbone temperature variation from core body	40
Fig. 1.13 – Ostrich $\delta^{18}\text{O}_{\text{phosphate}}$ per bone	41
Fig. 1.14 – Ostrich intrabone temperature variation	42
Fig. 1.15 – Ostrich interbone temperature variation	43
Fig. 1.16 – Ostrich interbone temperature variation from core body	44
Fig. 2.1 – <i>Acrocanthosaurus</i> $\delta^{18}\text{O}_{\text{phosphate}}$ vs. $\delta^{18}\text{O}_{\text{carbonate}}$	61
Fig. 2.2 – <i>Acrocanthosaurus</i> standard deviation by bone type	62
Fig. 2.3 – <i>Acrocanthosaurus</i> $\delta^{18}\text{O}_{\text{phosphate}}$ vs. cement $\delta^{18}\text{O}_{\text{carbonate}}$	63
Fig. 2.4 – <i>Acrocanthosaurus</i> $\delta^{18}\text{O}_{\text{phosphate}}$ per bone	64
Fig. 2.5 – <i>Acrocanthosaurus</i> intrabone temperature variation	65
Fig. 2.6 – <i>Acrocanthosaurus</i> interbone temperature variation	66
Fig. 2.7 – <i>Acrocanthosaurus</i> interbone temperature variation from core body	67
Fig. 2.8 – Phosphate $\delta^{18}\text{O}$ ranges	68

Introduction

Dinosaurs represent one of the most unique groups of animals to have lived on earth. Their plethora of sizes, morphologies, and lifestyles serve as a constant source of inspiration for new and innovative research. A long-standing point of debate surrounding these creatures concerns their metabolic functioning and thermoregulatory status. The large size and potentially active lifestyle of some species lead to questions concerning the necessary metabolic requirements. There has been a trend in recent studies towards a more chemical and/or technological approach to this problem (Barrick and Showers 1994, 1995, 1996, 1999; Barrick et al. 1998; Fricke and Rogers 2000). This study focuses on one species of large carnivore, *Acrocanthosaurus atokensis*, in an effort to categorize its method of thermoregulation using isotopic analyses.

TERMINOLOGY

Animals have applied numerous strategies to the regulation of their body temperatures. This study follows Bligh and Johnson (1973) for definition of thermophysiology terms. The first basic distinction is tachymetabolism versus bradymetabolism. Tachymetabolic organisms maintain a high level of basal metabolism; bradymetabolic organisms have a lower basal level. An extension of these two distinctions is heterothermy versus homeothermy, both referring to temperature regulation in tachymetabolic animals. Homeothermy refers to cyclic variations in the

core body temperature that are maintained within arbitrarily defined limits (usually approximately $\pm 2^{\circ}\text{C}$), whereas heterothermy refers to variations in the core body temperature that exceed the defined limits of the former. A special case of heterothermy is often termed poikilothermy. Organisms employing this method of thermoregulation experience large variability in core body temperature as a proportional function of the ambient temperature. They are more generally described as “temperature conformers” because their body temperatures usually equal the ambient temperatures. It should be noted that poikilothermy differs from bradymetabolism in that the latter does not necessarily experience this equality between body and ambient temperature. The method of temperature regulation (or lack thereof) further distinguishes an animal. Endothermic organisms maintain their body temperature through a high (tachymetabolic) and controlled metabolism. In addition to their naturally high metabolic rate, their bodies have the ability to initiate metabolism of energy reserves through biochemical feedback mechanisms and distribute the resulting heat by increasing heart rate and circulation. Ectotherms do not possess a metabolic rate capable of maintaining constant temperature. Instead, they rely on behaviorally or autonomically regulated uptake of heat from the environment.

Combinations of the above-listed strategies produce some of the more common thermophysiological terms. A classic “warm-blooded” organism is more properly categorized as a homeothermic endotherm. This study will continue its reference to Bligh and Johnson (1973) and consider warm-blooded organisms as those animals that

maintain a core body temperature higher than that of the environment when subjected to low ambient temperatures. A “cold-blooded” organism is one that allows its core body temperature to remain close to ambient when subjected to low ambient temperatures. According to the previous definitions, cold-blooded animals are therefore both heterothermic and ectothermic. They also tend to be bradymetabolic and conform to the special case of poikilothermy. "Behaviorally adaptative homeotherms" maintain a constant body temperature through specific behaviors such as solar basking, panting, shade-seeking, etc. The use of homeothermy in this description is slightly misleading as these animals do not employ tachymetabolism (a previously defined condition for homeothermy). These types of organisms are more appropriately and hereafter referred to as behavioral temperature regulators. "Gigantotherms" are best described as ectothermic temperature regulators capable of maintaining constant body temperature due to a high body mass that in essence buffers excessive heat loss or gain. This term is often described as ectothermic homeothermy. However, this study will avoid the use of homeothermy in reference to gigantotherms as it is again an inappropriate use of the term homeothermy. Finally, "regional heterothermy" is a plan where the temperature of certain body parts (usually the extremities) varies to a greater degree than the core body. In this plan, the core body maintains a homeothermic condition (i.e. variation within +/- 2°C).

PREVIOUS RESEARCH

Previous research focusing on dinosaurian metabolism has employed a number of different methods resulting in a variety of conclusions. Mathematical modeling of extant reptiles applied to the extinct dinosaurs suggests that gigantothermy would be a beneficial and viable possibility (Paladino et al. 1990, Spotila et al. 1973). Low metabolic rate coupled with large body size would facilitate survival in fluctuating daily temperatures or fluctuating seasonal temperatures during hypothetical migrations. Furthermore, this thermoregulatory strategy would allow an organism to live in harsher, colder climates due to the thermal inertia of a larger body mass. Computer modeling suggests the need for variety of thermoregulatory strategies in response to different thermal problems encountered at either end of the body size continuum (O’Conner and Dodson 1999, Spotila et al. 1991). Smaller sized dinosaurs (~ <10kg) would not benefit greatly from metabolically enhanced heat production unless they possessed insulation of some sort. However, they would benefit from behavioral selection of microhabitats to accommodate changing daily or seasonal temperatures. Larger dinosaurs would experience the opposite scenario where behavioral adaptation is of little use due to their larger mass buffering rapid heat loss or gain from the environment (i.e. gigantothermy). In this case, the larger mass would also provide enough insulation to retain metabolically produced heat. Furthermore, tachymetabolic rates may have put larger dinosaurs at risk of overheating. The suggestion from these previous studies then remains that dinosaurs employed an intermediate rate of metabolism, or they may have in fact been highly skilled endotherms

that could vary their metabolic heat production throughout their daily, seasonal, and lifetime cycles.

Several potential contradictions arise here. Gigantothermy implies a bradymetabolic, and therefore unstable body temperature, throughout the early life-stages before the animal is large enough to buffer heat loss and gain. Growth rates should then be higher in the adult stage when body temperatures are higher and stable. However, examination of various dinosaur species has yielded patterns showing high growth rates similar to mammals early in life with a tapering in later stages (Erickson et al. 2001, Padian et al. 2001). This conundrum could be resolved if dinosaurs employed endothermic metabolism in the juvenile stage with a later shift to a lower mass specific metabolism at larger sizes.

A strict morphological approach arrives at slightly different conclusions, but is also subject to controversy and contradictions. Analysis of the cross-sectional area of the nasal passages suggests that some theropod dinosaurs and at least one ornithischian exhibited the more restricted passageways characteristic of lizards and crocodiles as opposed to mammals (Ruben et al. 1996). These dinosaurs then would have been incapable of supporting endothermic ventilation rates, but may still have been capable of a metabolism slightly higher than modern ectotherms. However, Horner (1995) and Brochu (2003) suggest that hadrosaurs, ceratopsians, and possibly theropods had large corrugated narial chambers capable of supporting cartilaginous turbinates. These structures primarily control water loss during ventilation, yet they are absent or extremely

reduced in some modern birds and primates (Paul 1995). The question then remains whether the need for narial turbinates is controlled by metabolic rate or by temperature and humidity of the climate. The use of these structures as thermoregulatory indicators is still tenuous.

Examination of sauropod neck posture, the associated blood pressures, and the stress on the ventricular wall suggests that an endothermic metabolism would severely limit the potential postures for this group of dinosaurs (Seymour and Lillywhite 2000). Pressure associated with the raising of the head, coupled with the relatively rapid heart rate necessary for maintenance of endothermy, would be overwhelming for the hypothesized physiology of the sauropods. An ectothermic metabolism appears to support a smaller heart size and a more restricted variety of neck postures. However, heart size is not correlated to physiology, but rather to body size. Lizards, mammals, and birds of the same body size have the same heart size.

Recently, a geochemical approach has been applied in an attempt to acquire more detailed quantitative constraints for thermoregulation within dinosaurs. Specifically, researchers are examining the oxygen isotope signatures (i.e. $\delta^{18}\text{O}$) from the phosphate in dinosaur bones and teeth (Barrick and Showers 1994, 1995, 1996, 1999; Barrick et al. 1998; Fricke and Rogers 2000). The basic premise behind this approach is the temperature dependence of the oxygen isotope fractionation factor between phosphate in mineralizing bones or teeth and the oxygen source for that phosphate. Therefore animals using different metabolic strategies should show different isotopic signatures. Longinelli

and Nuti (1973) used marine shell data to develop the following equation relating the phosphate oxygen isotope signature ($\delta^{18}\text{O}_{\text{ph}}$) to the environmental temperature (T) and the environmental oxygen isotope values ($\delta^{18}\text{O}_{\text{w}}$):

$$T = 111.4 - 4.3(\delta^{18}\text{O}_{\text{ph}} - \delta^{18}\text{O}_{\text{w}})$$

The equation's slope indicates that for every 1 permil increase in $\delta^{18}\text{O}_{\text{ph}}$, there is a 4.3°C decrease in the temperature of formation. Data suggest that this slope is applicable to vertebrates as well as marine invertebrates (Luz and Kolodny 1985, D'Angela and Longinelli 1990). A direct correlation exists between the $\delta^{18}\text{O}$ value of the environmental water and the $\delta^{18}\text{O}$ value of the body water (Longinelli 1984, Luz and Kolodny 1985, Luz and Kolodny 1989) thus allowing the latter to replace the former in the paleotemperature equation when applied to vertebrates. Therefore, in the absence of environmental data (as is the case with most fossil dinosaur specimens), one can multiply interbone or intrabone isotopic differences by 4.3 to arrive at maximum temperature variation within the animal. This method allows a very detailed analysis of heat differences within the parts of one individual body, thereby distinguishing between homeothermy, heterothermy, and regional heterothermy.

Thus far these studies have yielded evidence of a warm-blooded nature for the dinosaurs that have been sampled. Barrick and Showers (1994) found intrabone and interbone isotopic variability in a *Tyrannosaurus rex* specimen that indicated thermal variation of less than 4°C, which suggests homeothermy. Small intrabone and interbone

variability in *Hypacrosaurus* juveniles suggested homeothermy and endothermy as well (Barrick and Showers 1995). The $\delta^{18}\text{O}$ values of four ornithischians from the Two Medicine Formation again indicated low thermal variability and a high probability of homeothermy (Barrick and Showers 1996). Compared to these same ornithischians, a varanid lizard exhibited high thermal variability indicative of heterothermy. Barrick et al. (1998) examined the frill and horn of a *Triceratops* specimen ultimately concluding that these structures were important in maintaining a homeothermic state in the body and stabilizing brain temperatures. A later comparison between *Giganotosaurus carolinii* and *T. rex* found that the former also supported homeothermy through use of an intermediate metabolic rate (Barrick and Showers 1999). Fricke and Rogers (2000) compared $\delta^{18}\text{O}$ values from theropod teeth at different latitudes in an effort to obtain the $\delta^{18}\text{O}_{\text{tooth enamel}}$ vs. latitude relationship (a correlation which is theoretically dependant primarily on the method of thermoregulation). The observed relationship most closely resembled that of modern day birds and mammals as opposed to crocodilians, therefore suggesting homeothermic warm-blooded dinosaurs.

To date, only Barrick and Showers (1994, 1999) have examined theropod dinosaur skeletons using this isotopic method. The theropods present interesting cases as they are carnivorous and potentially active predators. Questions concerning their roles as active predators versus slower scavenging animals often rely on the animals' abilities, or lack thereof, to metabolically maintain an active lifestyle. Furthermore, a large theropod might require supplemental thermoregulatory adaptations depending on its environment.

For example, a large active predator in a predominantly hot climate may require special adaptations to accommodate the increased body temperatures resulting from its lifestyle and ecosystem. Some possibilities suggested by studies of modern large carnivores such as crocodylians include oral gaping, gular pumping, vascular shunting, or locomotory thermogenesis (Smith 1979, Bartholomew 1982, Huey 1982, Turner and Tracey 1983). While a geochemical analysis cannot be used to examine all of these possibilities, it will indicate any temperature differences present between different body parts. Isotopic data from localized areas, such as the palate and braincase, should then indicate behaviors such as gaping or shunting that produce such differences. This more precise examination of temperature variation coupled with the determination of general metabolic strategy and other morphological inferences could potentially reveal behavioral patterns in these large carnivores.

OBJECTIVES

This study focuses on *Acrocanthosaurus atokensis* as a subject for isotopic and thermoregulatory study. *A. atokensis* is an allosauroid carnosaur currently known from only four specimens found in the south central United States. The type specimen and paratype were found in Oklahoma sandstones of the Trinity Group dated to be Aptian-Albian in age (~121-99Ma) (Stovall and Langston 1950). A third specimen was found in Texas sandstones of the Twin Mountains Formation (lowest member of the Trinity Group) dated as late Aptian (~118-112Ma) (Harris 1998). The fourth specimen was

acquired from Oklahoma sandstones of the Antlers Formation (correlated to the lower part of the Twin Mountains Formation) and is also considered to be Aptian-Albian in age (Currie and Carpenter 2000). The Antlers Formation is composed primarily of fluvial sandstones, siltstones, and mudstones (Hobday and McKalips 1979, Winkler et al. 1989). The lithology indicates a seasonally dry climate as do the recovered fern, cycad, and conifer species that are commonly found in poor dry soils (Winkler et al. 1989). This study is based on the latter specimen that is now repositied at the North Carolina State Museum of Natural History (specimen NCSM 14345).

A. atokensis proves to be an interesting subject due to its large size (estimated 2400kg by Currie and Carpenter 2000), unique morphological features, and environment of origin. The Antlers Formation represents a near shore fluvial environment during the Aptian-Albian (Jacobs et al. 1991, Hobday and Mckalips 1979, Michael 1972). This time period is characterized by the rise of a hot-house climate with warmer sea-surface temperatures and reduced latitudinal gradients that eventually culminated in the Cenomanian (Huber et al. 2002, Wilson and Norris 2001, Fassell and Bralower 1999, Huber et al. 1995, Barron 1983). *A. atokensis* is clearly a carnivore and possibly a very active one as evidenced by its tooth structure, large yet agile body, robust manus and pes, and broad surfaces for muscular articulation in the pelvic region (Harris 1998, Currie and Carpenter 2000). A combination of environment and body morphology suggests that *Acrocanthosaurus* required a moderate to high metabolism to maintain activity as well as mechanisms to reduce the risk of overheating. This species possessed broad and high

neural spines, the increased external surface area of which may have been used as a heat exchanging mechanism. The palate and braincase of NCSM 14345 are exceptionally well preserved. The palate could be another heat exchange surface while any temperature differences between the body and the braincase might suggest preferential temperature regulation of only certain body parts.

Modern animals representing a cross section of body sizes, morphologies, and thermoregulatory strategies were analyzed to provide a more complete picture of how the $\delta^{18}\text{O}$ values vary with these strategies and then to provide a basis for the interpretation of the *Acrocanthosaurus* data. An elephant represents large homeothermic endotherms, alligators represent bradymetabolic ectotherms, and ostriches represent homeothermic endothermic descendants of theropods. This study postulates the maintenance of an intermediate to full homeothermic condition in *A. atokensis*. Furthermore, this condition is maintained by partial to full endothermy with morphologic mechanisms to prevent overheating.

Chapter 1 – Examination of Modern Animals

Modern animals are used here to both examine the fossil specimens for diagenesis and serve as a means for comparison with the *Acrocanthosaurus atokensis* material.

MATERIALS AND METHODS

An ostrich specimen, *Struthio camelus* (NCSU-OS1), raised at the North Carolina State University School of Veterinary Medicine was stripped of fleshy material during a one year burial when natural organic decomposition processes were allowed to remove the soft tissues.

Various bones of two different *Alligator mississippiensis* specimens were obtained. NCSU#2-94 is a Florida specimen that was farm raised at a temperature of 32°C. Oxygen isotope values from this specimen have previously been published in Stoskopf et al. (2001). Specimen NCSU-G7 was obtained from the North Carolina State University zoology collections. It was originally a wild individual from the North Carolina area.

One elephant was obtained from the North Carolina State University School of Veterinary Medicine (specimen NCSU-E1). In life it was housed at the North Carolina Zoo.

A small amount of powder (~30-50mg) was drilled from various sites on each bone using a common rotary tool with an engraving bit. The sampled bones encompass

all the major body regions (i.e. core body, limbs, tail, and head if available). Regions with long bones were sampled at approximately evenly spaced intervals along the bone's length in an effort to obtain temperature variation at intervals from the core to the most distal regions. Drill sites were selected from areas with minimal physical degradation (i.e. cracking or loss of layers). Each drill site consisted of individual samples taken at several depths encompassing both cancellous and compact bone. This strategy allows for temperature comparison within a bone. The bone powders were then processed for phosphate and carbonate isotope analysis according to the procedures outlined in the following sections.

Phosphate oxygen isotopes:

Bone phosphate was isolated from all modern material according to procedures described in Dettman et al. (2001). Approximately 5-10mg of sample powder was reacted overnight at room temperature in 1mL of 2M hydrofluoric acid. Four mL of deionized water was added, the mixture centrifuged, and the supernatant saved. The supernatant from a second 5mL rinse of the residual powder was added to the first. The resulting 10mL of supernatant was buffered with 0.8mL of 20% ammonium hydroxide solution. One mL of 2M silver nitrate solution was added and the resulting silver phosphate precipitate was washed with three separate deionized water rinses where the supernatant after centrifuging was discarded. The remaining solid was dried for two days at ~100°C.

Approximately 500µg of silver phosphate powder was loaded into a small combustible silver boat for each sample (3.5 x 5 mm, Costech, Valencia, CA). The samples were then analyzed using a Thermo Finnigan (Brennan, Germany) DELTA^{plus}XL dual inlet/continuous flow isotope ratio mass spectrometer coupled to a Thermo Finnigan TC/EA (thermo-chemical elemental analyzer). At a reaction temperature of 1450°C in contact with glassy carbon, the oxygen in the silver phosphate is converted to carbon monoxide. The resulting gases from the combustion reaction, including the CO, are separated in a gas chromatograph column of 5A mole sieve held at 85°C. Once separated, the CO is admitted to the isotope ratio mass spectrometer and referenced against an internal reference CO gas (Messer, Duisberg, Germany; -5.5+/- 2.0‰ δ¹⁸O vs V-SMOW) admitted through the dual inlet bellow. Raw data are normalized using sucrose ANU (NBS RM 8542), an internal sucrose standard, and three internal silver phosphate standards of known value, previously normalized against NBS-127 barium sulfate (NBS RM 8557) and sucrose ANU. Isotopic values are reported relative to V-SMOW in the standard δ notation where $\delta^{18}\text{O} = [(R_{\text{sample}}/R_{\text{standard}}) - 1] * 1000$ and $R = {}^{18}\text{O}/{}^{16}\text{O}$.

Carbonate oxygen and carbon isotopes:

Bone carbonate was isolated from all modern material according to a modification of the procedures of Bryant et al. (1996). Approximately 5mg of sample powder was reacted overnight in a 2-3% sodium hypochlorite solution at room temperature to remove

any organic carbon compounds. The remaining powder was rinsed three times with deionized water and dried for two days at ~100°C.

All $\delta^{18}\text{O}$ and $\delta^{13}\text{C}$ values of the dried powder were measured on a Micromass (Manchester, UK) dual inlet/continuous flow isotope ratio mass spectrometer coupled to a Micromass Multiprep carbonate analysis apparatus. Approximately 500-800 μg of powder was reacted with 100% phosphoric acid at 90°C in a vial under high vacuum. An aliquot of the released CO_2 was then injected into the mass spectrometer through a Gilson needle autosampler, cryogenically purified in a liquid nitrogen trap, and referenced against an internal CO_2 gas admitted via the dual inlet bellow in the mass spectrometer.

Oxygen isotopic values are reported relative to V-SMOW in the standard δ notation. $\delta^{18}\text{O} = [(\text{R}_{\text{sample}}/\text{R}_{\text{standard}}) - 1] * 1000$ where $\text{R} = ^{18}\text{O}/^{16}\text{O}$. Carbon isotopic values are reported relative to V-PDB. $\delta^{13}\text{C} = [(\text{R}_{\text{sample}}/\text{R}_{\text{standard}}) - 1] * 1000$ where $\text{R} = ^{13}\text{C}/^{12}\text{C}$.

Standards:

The precision of $\delta^{18}\text{O}$ values from phosphates was monitored by four standards. A wet chemistry laboratory standard (NAP) produced from 0.1M $\text{Na}_2\text{HPO}_4 \cdot 7\text{H}_2\text{O}$ solution was processed through the same procedure as the bone samples. The resulting precipitate yielded $\delta^{18}\text{O}$ values ± 0.13 permil (1σ). The mass spectrometry laboratory also used three in-house standards. AASP is an Alpha Aldrich (Ward Hill, MA) phosphate standard yielding $\delta^{18}\text{O}$ values ± 0.23 permil (1σ). SASP is an Alpha Aesar

(Milwaukee, WI) phosphate standard yielding $\delta^{18}\text{O}$ values ± 0.24 permil (1σ). Finally, a laboratory sucrose standard yielded $\delta^{18}\text{O}$ values ± 0.25 permil (1σ).

Precision of $\delta^{18}\text{O}$ and $\delta^{13}\text{C}$ values from the carbonates was monitored by the house standard LL1. This is a pure carbonate rock from the Lincoln Limestone that has been calibrated with instrumentation at Harvard University to NBS-19, a NIST standard originally calibrated to the Peedee Belemnite (PDB). The LL1 standard yielded $\delta^{13}\text{C}$ values ± 0.052 permil (1σ) and $\delta^{18}\text{O}$ values ± 0.095 permil (1σ).

RESULTS AND DISCUSSION

Implications to fossil diagenesis:

Data from this study seem to contradict previous research, indicating that phosphate and carbonate oxygen isotope values of unaltered bones do not correlate. Previous research has suggested that bones unaffected by post mortem diagenesis should exhibit $\delta^{18}\text{O}_{\text{phosphate}}$ and $\delta^{18}\text{O}_{\text{carbonate}}$ values with a strong positive linear correlation (Iacumin et al. 1996, Bryant et al. 1996). These studies assume that vital effects responsible for fractionating oxygen into the two different ions function in similar ways. In mammals, the carbonate is usually more enriched in ^{18}O than the phosphate by $\sim 8.5\%$ (Bryant et al. 1996). The literature has yet to demonstrate that this is also true for ectothermic animals.

In this study, the homeothermic endotherms (i.e. the ostrich and elephant) show no correlation between $\delta^{18}\text{O}_{\text{phosphate}}$ and $\delta^{18}\text{O}_{\text{carbonate}}$ values (Figs. 1.1 and 1.2). The Pearson correlation coefficients for the ostrich and elephant were 0.226 and 0.105, respectively. The phosphate values exhibit a rather small range of values (2.8‰ for the ostrich and 1.5‰ for the elephant). The carbonates vary to a much greater degree (7.2‰ for the ostrich and 10.7‰ for the elephant). The ectothermic heterotherm (i.e. the alligator) also showed a lack of correlation ($p = 0.272$) between $\delta^{18}\text{O}_{\text{phosphate}}$ and $\delta^{18}\text{O}_{\text{carbonate}}$ values (Fig. 1.3). The phosphate values had a range of 3.5‰ while the carbonates had a range of 7.1‰.

None of the data agree with the previously published separation of 8.5‰ between the two ions. This suggests that vital effects on oxygen isotopic fractionation in mammal bones are different for carbonate versus phosphate. The isotopic value of inhaled CO₂ may not in fact be in equilibrium with the blood. As CO₃ is extracted from mineralized bones for various body functions (eg. CO₂ buffering of blood chemistry), fractionation may occur. Carbonate in body fluids is metabolically active and may interact with the structural carbonate in the bone apatite, shifting oxygen isotopes in the latter from their original values. Fractionation of the structural carbonate might not be consistent among the different bones of the body.

Modern reptiles and birds do not appear to conform to the same pattern as mammals (i.e. different patterns of temperature variation and isotopic ranges throughout the body). While this study suggests that bones unaffected by post mortem diagenesis will not necessarily exhibit $\delta^{18}\text{O}_{\text{phosphate}}$ and $\delta^{18}\text{O}_{\text{carbonate}}$ values in a direct linear relationship, the more important pattern shown by unaltered bones is the range of phosphate values compared to those of carbonate values. All the modern animals showed a lower variance amongst the $\delta^{18}\text{O}_{\text{phosphate}}$ values as compared to the $\delta^{18}\text{O}_{\text{carbonate}}$ values ($p < 0.01$). As evidenced by these modern animals, unaltered fossil bones should show a narrower range of oxygen isotope values in phosphate than in carbonates. Thus a linear correlation between $\delta^{18}\text{O}_{\text{phosphate}}$ and $\delta^{18}\text{O}_{\text{carbonate}}$ is more likely representative of diagenetic alteration than it is of preservation as suggested by Iacumin et al. (1996).

In addition to the linear relationship between $\delta^{18}\text{O}_{\text{phosphate}}$ and $\delta^{18}\text{O}_{\text{carbonate}}$ (or lack thereof), one must consider the variation of values by bone type (Fig. 1.4). The alligator and the elephant show little or no variation in $\delta^{18}\text{O}_{\text{phosphate}}$ between compact and spongy bone. A comparison of the standard deviations in the δ -values associated with each bone type (alligator $n_{\text{compact}} = 20$ and $n_{\text{spongy}} = 12$; elephant $n_{\text{compact}} = 18$ and $n_{\text{spongy}} = 15$) produced no significant differences ($p > 0.1$ for both animals). The alligator showed standard deviations in the spongy bone that were slightly lower than that of the compact bone. The elephant showed the opposite pattern. The ostrich showed a standard deviation in the spongy bone ($n = 7$) that was relatively lower than that of the compact bone ($n = 27$), yet there was no statistically significant difference at a α value of 0.05 ($p = 0.05-0.1$). One would then expect to see the standard deviations within the two bone types to be statistically similar for isotopically unaltered fossil bone. Altered bones would be expected to show a higher standard deviation within the spongy bone as it is more porous and susceptible to groundwater infiltration and subsequent isotopic alteration.

Examination of thermoregulation:

Alligator

The alligator exhibits a logical pattern of thermal variation for an ectothermic heterotherm experiencing a lack of precise control over its body temperature. The range in values for each individual site varies by bone (Fig. 1.5). The greatest amount of

variation occurs in the dorsal vertebra and the least amount occurs in the maxilla. The remaining bones display approximately similar ranges although the δ -values themselves differ markedly. The δ -values of the skull bones are notably lower than those of the main body. The actual temperature variation within each individual bone is shown in Fig. 1.6. This temperature variation is calculated by a multiplication of the aforementioned ranges with the slope value from the paleotemperature equation (i.e. 4.3). As a result, the dorsal vertebra exhibits the greatest amount of temperature variation while the maxilla exhibits the least. It is necessary to note here that the largest apparent temperature range of $\sim 15^{\circ}\text{C}$ is primarily a function of two extreme data points. However, these points do not appear as statistical outliers according to SAS software analyses (specifically studentized residuals, Hat Matrices, DFFITS, DFBETAS, and Cook's D). There is no discernable pattern to the remaining bones. This, however, is typical for alligators as they cannot entirely control their body temperature.

Temperature differences between bones can be compared by plotting calculated bone temperature normalized to the warmest bone in the individual (Fig. 1.7). In this instance the head and the main body are treated as two separate entities. The dentary and the femur prove to be the warmest bones of the head and body, respectively. The remaining bones vary in no discernable pattern. The maximum interbone temperature difference occurs in the maxilla (8.6°C). Interestingly, the head bones seem to vary more than the body bones. The palatine shows the least amount of temperature change from the chosen zero point, which may be a result of the alligator's use of oral gaping as a

method of temperature regulation. The palatine appears slightly warmer than all the bones (including the main body) except the dentary. The cause for such a pattern could be a preferential shunting of warm blood to the area in an attempt to lose as much heat as possible during oral gaping.

A comparison of temperature differences between bones using a core bone of the body as the zero point produces several interesting observations (Fig. 1.8). Most notable is that the temperatures for the main body seem to stay within the predefined limits for homeothermy (i.e. +/- 4°C). However, bones very close to one another show little consistency of temperature. The two dorsal vertebrae differ by at least 1.5°C. The humerus and the femur, both approximately the same distance from the core body, differ by almost 4°C. The phalange and the two caudal vertebrae, all of which are at the most distal parts of the body, show variation in their temperature differences as well.

Additionally, all the bones except the humerus appear to be warmer than the dorsal vertebra used as the zero point. Stoskopf et al. (2001) noted the same pattern and suggested the core body might experience a lower temperature due to extensive water loss at the extremities (Davis et al. 1980) resulting in cool blood returning to the core. These data may fall within the bounds of homeothermy due to the fact that this alligator was farm-raised at a constant temperature. However, the lack of any pattern in interbone temperature variation suggests a lack of temperature control across individual elements of the body. This seems logical for an ectothermic animal.

Elephant

The elephant exhibits a logical pattern of temperature variation for an endothermic homeotherm capable of a more precise control of its body temperature. As with the alligator, the range of values for each individual site varies by bone (Fig. 1.9). The femur exhibits the greatest variation and the metatarsal the least. The remaining bones show approximately equal ranges and δ -values; the one exception being the caudal vertebra. The actual calculation of temperature variation taken from these ranges is shown in Fig. 1.10. Excluding the femur, none of the bones vary beyond 4°C. This is an expected condition for a large endotherm that has the ability to maintain a constant body temperature and likely faces greater stress for heat dumping rather than conservation. The femur is in a location where it does not experience the mass buffering effect of the main body. Nor does it experience the conductive warming from the ground that has been noted in thermographic scans of elephant skin surface temperatures (Williams 1990). This apparent lack of temperature buffering might explain the anomalous intrabone temperature variation within the femur.

A comparison of temperature differences between the bones using the warmest bone as a zero point is shown in Fig. 1.11. This analysis suggests that the warmest bone is the distal portion of a rib. The bones most similar in temperature to this one are the proximal portion of the same rib and the femur. The interbone temperature difference increases distally culminating in the caudal vertebra showing the most variation from the

core body. Such a pattern is expected since elephants' caudal vertebrae are protected by only a thin layer of flesh on a very thin tail.

A comparison of interbone temperature variation using a core body bone as a zero point provides further support for the homeothermic condition of elephants (Fig. 1.12). None of the bones, including the caudal, vary beyond 4°C of the core body (i.e. the lumbar vertebra). The ribs appear slightly warmer than the lumbar vertebrae most likely due to their location in the large, well insulated, highly metabolizing gut of the elephant. The leg bones are also slightly warmer than the lumbar and very similar to one another. The legs are insulated by flesh and have a somewhat uniformly cylindrical shape. These two factors work together to produce a uniform distribution of average temperature within the leg. It is notable that the femur exhibits very little variation from the other leg bones despite its individual intrabone variation. It lacks the temperature buffering of the core body or the ground at a given moment in time, yet it experiences the same average lifetime temperature variation as the other leg bones. The average temperature of the femur stays within the limits of homeothermy. The caudal vertebra appears to be cooler than the rest of the body. Again, this pattern is expected from the thin non-insulated tail of an elephant.

Ostrich

The ostrich shows slightly different patterns than the elephant. However, these patterns are readily explainable within the condition of endothermic homeothermy. The ranges of values for each individual site continue to vary between bones (Fig. 1.13). The femur and tibia show the greatest amount of intrabone variation while the dorsal vertebra, palatine, and vomer show the least. The calculation of intrabone temperature variation from these ranges reiterates this pattern (Fig. 1.14). The femur and tibia show an intrabone temperature variation beyond the 4°C limit of homeothermy. However, this is to be expected as the ostrich has very long, slender, and non-insulated legs. Infrared thermography has shown that ostrich leg temperatures tend to vary with the ambient temperature (Phillips and Sanborn 1994). At very low temperatures the animal is capable of keeping the legs at ~2.5°C above ambient. The core body, the head, and interestingly, the foot bones all stay within 4°C of variation. The body and the head (to a lesser degree) have better feather cover than the legs. Ostriches are known to reposition their feathers as a method of maintaining a preferred and fairly constant body temperature (Louw 1972, Phillips and Sanborn 1994). The head may also experience increased blood flow at times to aid in regulation of brain temperature.

The comparison of interbone temperature differences using the warmest bone as a zero point is shown in Fig. 1.15. The greatest deviations in temperature appear to occur in the bones of the head. A similar phenomenon is seen in the previously mentioned thermographic study of Phillips and Sanborn (1994). This is most likely due to the

diminished amount of insulation as compared to the rest of the body. The leg bones again show a significant amount of variation due to lack of insulation. Interestingly, the foot bone appears to be the warmest. This may be due to its direct contact with a warm substrate. Most of the bones stay within the 4°C limit for homeothermy. However, considering the warmth of the foot bone to be a special case, an examination of homeothermic bounds might not be appropriate here.

Comparing the interbone temperature variation using a core body bone as the zero point produces a more practical means for examining the homeothermic condition (Fig. 1.16). All the bones except the toe appear cooler than the core body (i.e. the dorsal vertebra). The warmth of the foot can again be explained by contact with a warm substrate. The remaining bones all appear to be cooler than the core body. This condition of regional heterothermy is expected for an animal with a round stout core and long slender appendages with high surface area that will not retain heat well. The dentary and palatine appear to be the coolest bones in the body. Their presence in the beak and subsequent lack of feathered insulation is the most likely factor responsible for this pattern.

CONCLUSIONS

While previous methods for the examination of fossil diagenesis are inconsistent with the current study, this analysis provides several methods to ascertain the integrity of fossilized phosphate oxygen isotopes. Specifically, an unaltered fossil specimen should exhibit a statistically insignificant linear correlation between $\delta^{18}\text{O}_{\text{phosphate}}$ and $\delta^{18}\text{O}_{\text{carbonate}}$ values, a tight range of $\delta^{18}\text{O}_{\text{phosphate}}$ as compared to $\delta^{18}\text{O}_{\text{carbonate}}$ values, and a difference between standard deviations of the compact and spongy bone $\delta^{18}\text{O}_{\text{phosphate}}$ values that is not statistically significant.

Determination of a dinosaur's thermoregulatory strategy can then be assessed by comparing it to the three modern species examined in this study. Intrabone and interbone temperature variations within all three species show some regional variation with specific patterns for each animal. The elephant and the ostrich primarily stay within the temperature bounds of homeothermy while the alligator does not. The elephant shows regional heterothermy in its tail and femur, while the ostrich exhibits regional heterothermy in its head and legs. However, consideration of the respective environments and varying insulation layers readily explains this regional body temperature variation within the endothermic homeotherm condition. Similar considerations explain the temperature pattern of the alligator within the ectothermic heterotherm condition. Analysis of a fossil specimen will therefore require examination

of interbone and intrabone variation in the context of living environment and body insulation.

FUTURE WORK

The applicability of modern animal isotopic data to the examination of diagenesis in a fossil specimen warrants clarification. Specifically, the observed lack of correlation between $\delta^{18}\text{O}_{\text{phosphate}}$ and $\delta^{18}\text{O}_{\text{carbonate}}$ values is a genuine observation, but is lacking explanation. A close tracing of oxygen isotopes through all the different compounds in the body is necessary, including the fate of oxygen after bone deposition. It is possible that there exists a stage of oxygen transfer within or between carbonates that is not an equilibrium reaction. A close analysis of growth rings might clarify if reworking of the bone throughout life is a source for fractionation due to carbonate exchange between blood and bone.

Overall, more modern studies of this nature will aid in building a database of isotopic information to which fossil specimens can be compared. Cranial elements in particular are often overlooked, but can provide valuable information concerning temperature patterns in an individual.

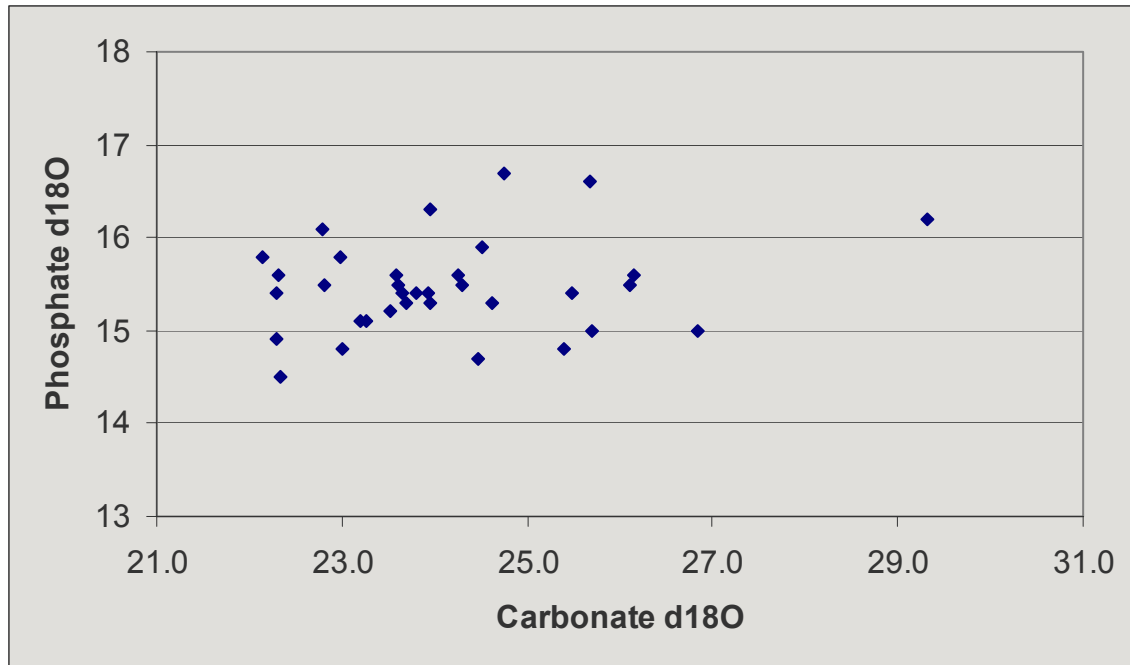


Figure 1.1 - Ostrich phosphate $\delta^{18}\text{O}$ versus carbonate $\delta^{18}\text{O}$ values. All values are reported in permil units relative to V-SMOW.

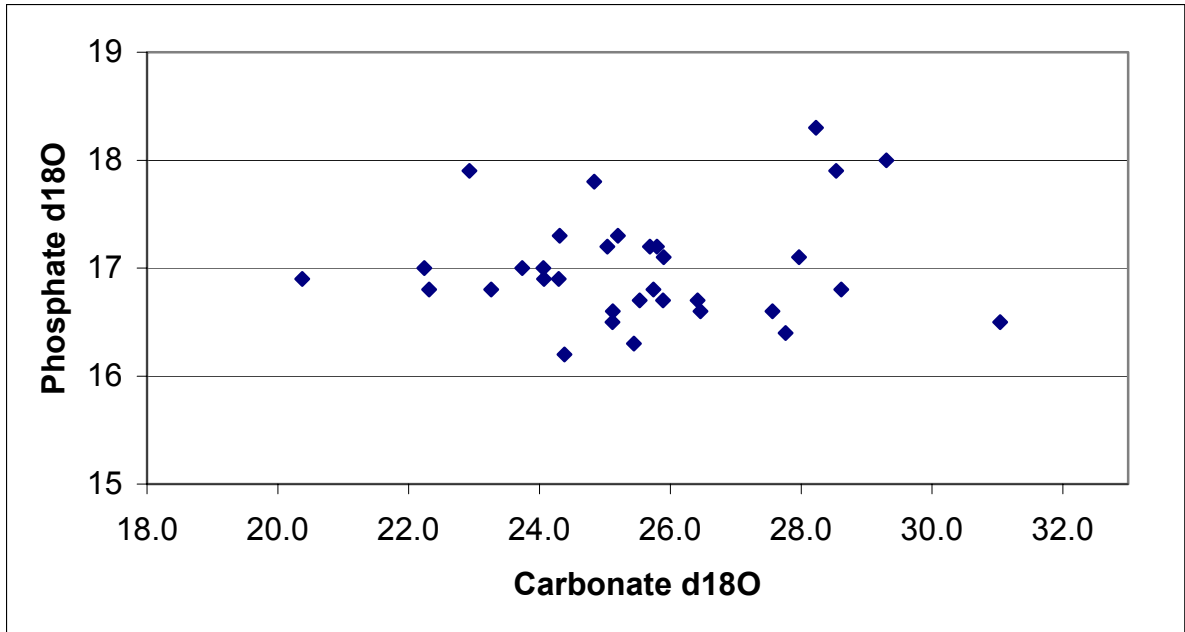


Figure 1.2 - Elephant phosphate $\delta^{18}\text{O}$ versus carbonate $\delta^{18}\text{O}$ values. All values are reported in permil units relative to V-SMOW.

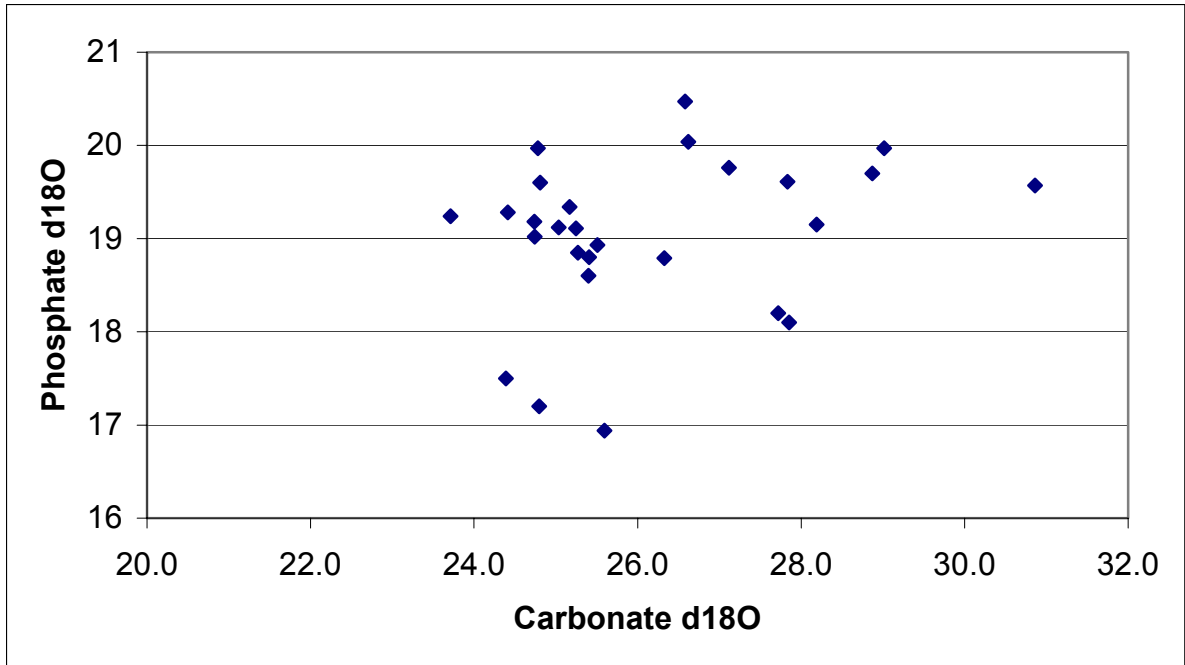


Figure 1.3 - Alligator phosphate $\delta^{18}\text{O}$ versus carbonate $\delta^{18}\text{O}$. All values are reported in permil units relative to V-SMOW.

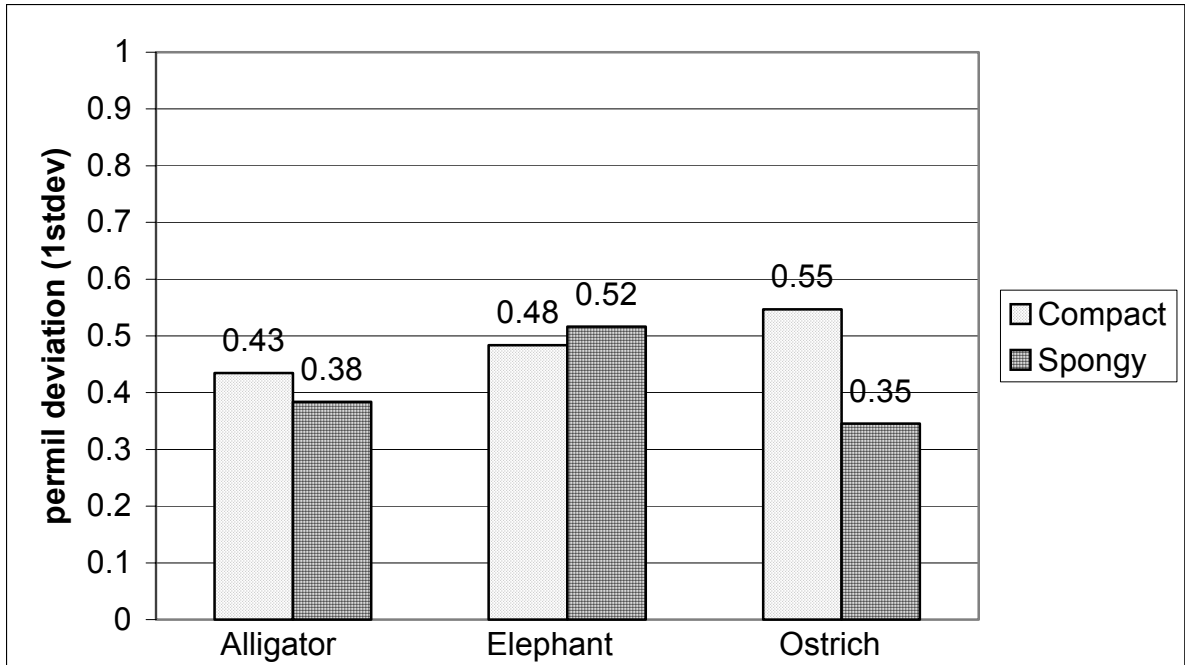


Figure 1.4 - Standard deviation of collected modern animal data for each bone type. Printed values represent one standard deviation from the mean.

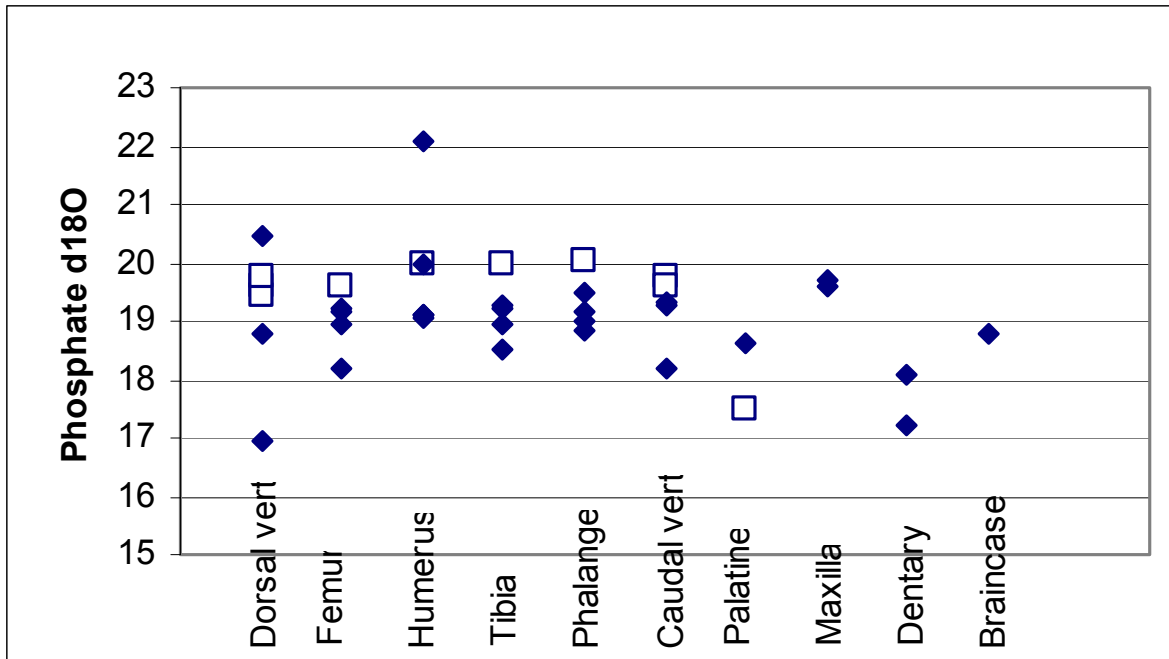


Figure 1.5 - Alligator phosphate $\delta^{18}\text{O}$ values for each bone. All values are reported in permil units relative to V-SMOW. Closed diamonds represent compact bone; open squares represent spongy bone.

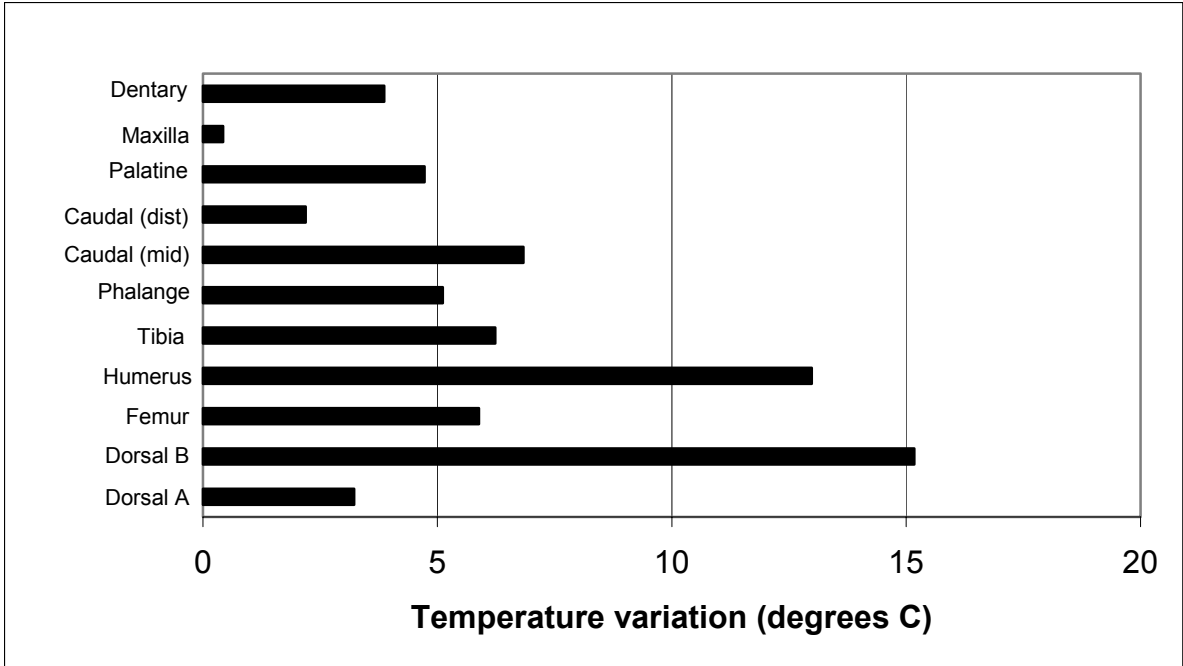


Figure 1.6 - Alligator intrabone temperature variation for each bone.

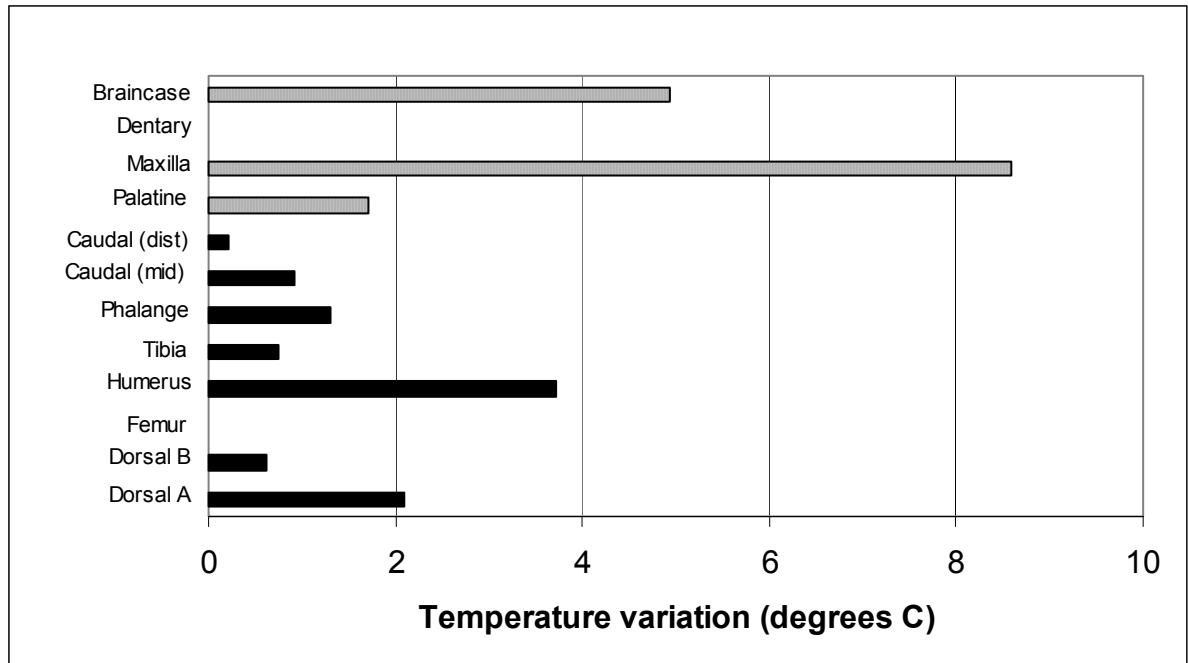


Figure 1.7 - Alligator interbone temperature variation based on the warmest bones in the body. Note that the cranial and body elements are treated as different individuals.

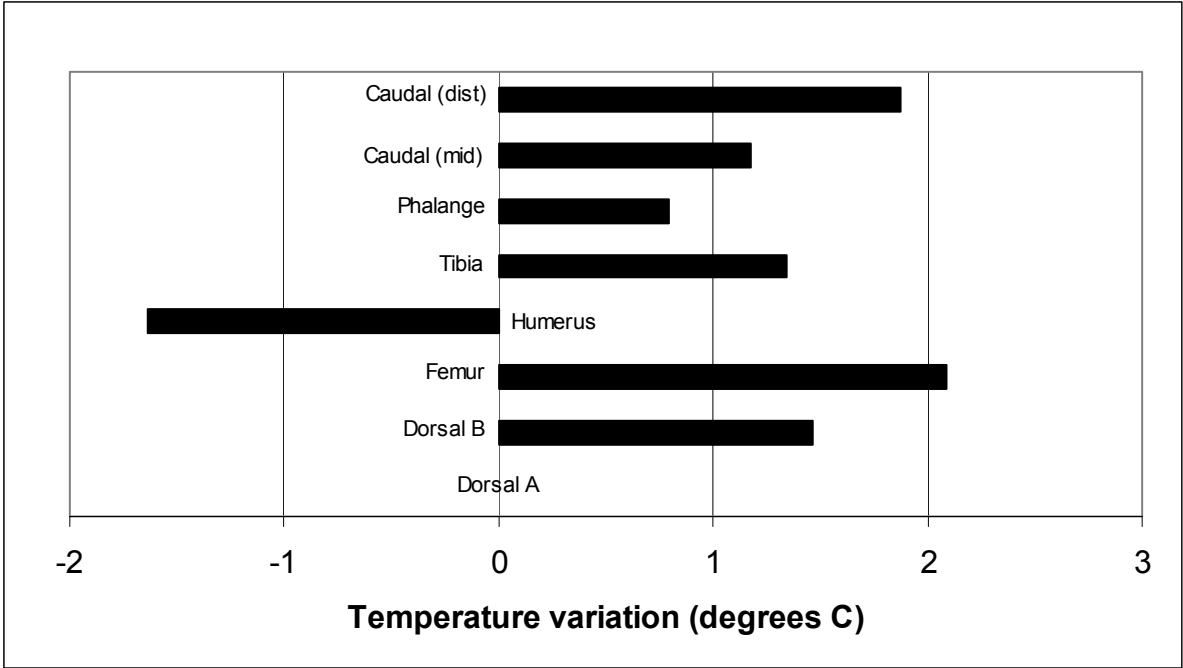


Figure 1.8 - Alligator interbone temperature variation from the core body.

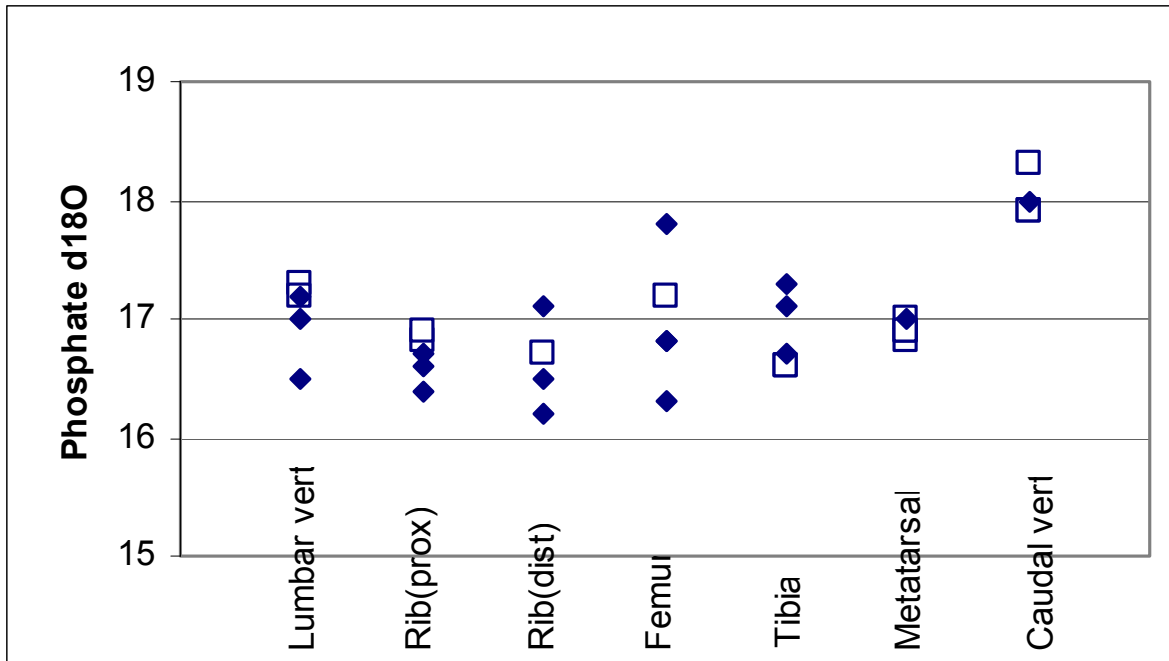


Figure 1.9 - Elephant phosphate $\delta^{18}\text{O}$ values for each bone. All values are reported in permil units relative to V-SMOW. Closed diamonds represent compact bone; open squares represent spongy bone.

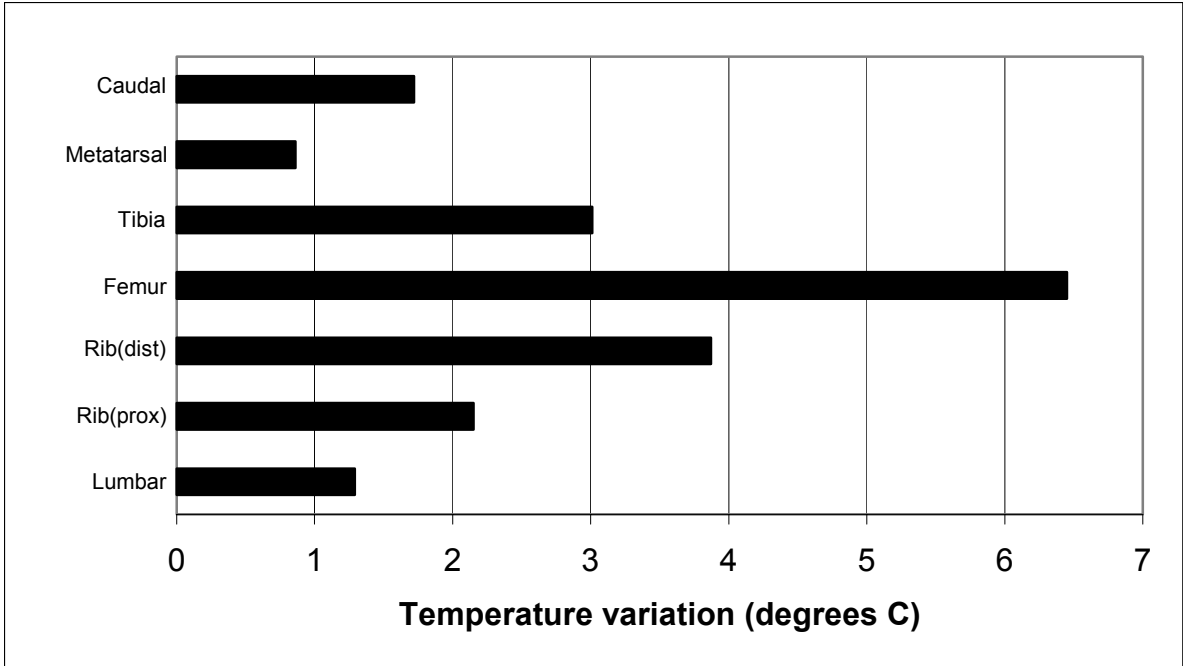


Figure 1.10 - Elephant intrabone temperature variation for each bone.

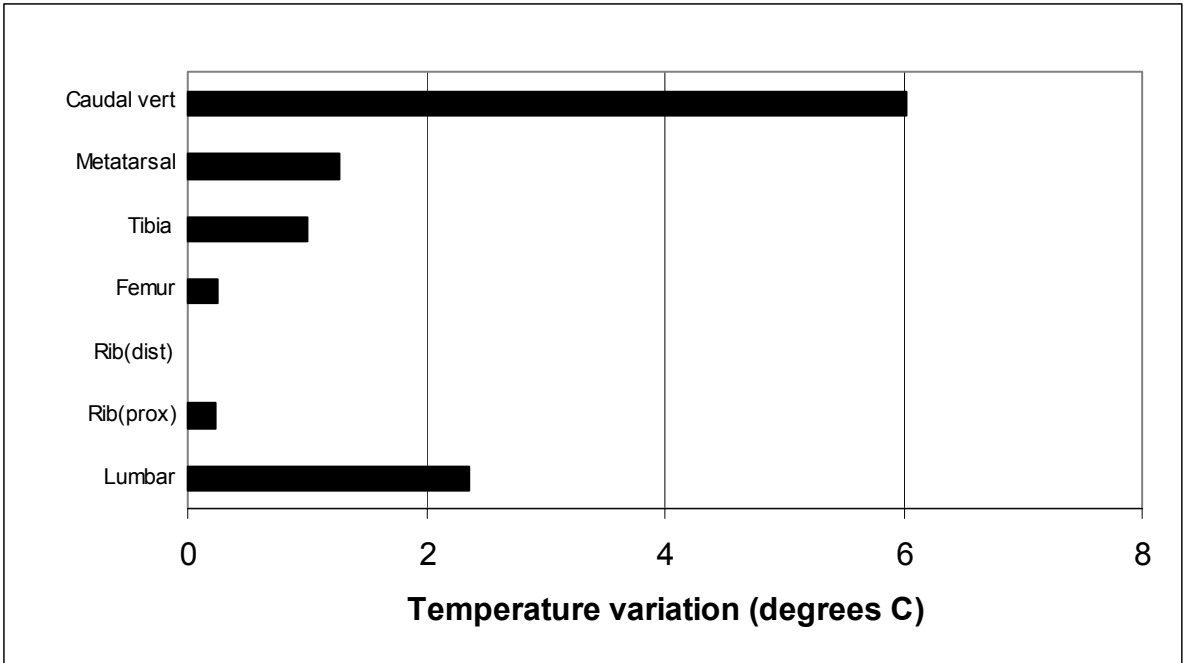


Figure 1.11 - Elephant interbone temperature variation based on the warmest bone in the body.

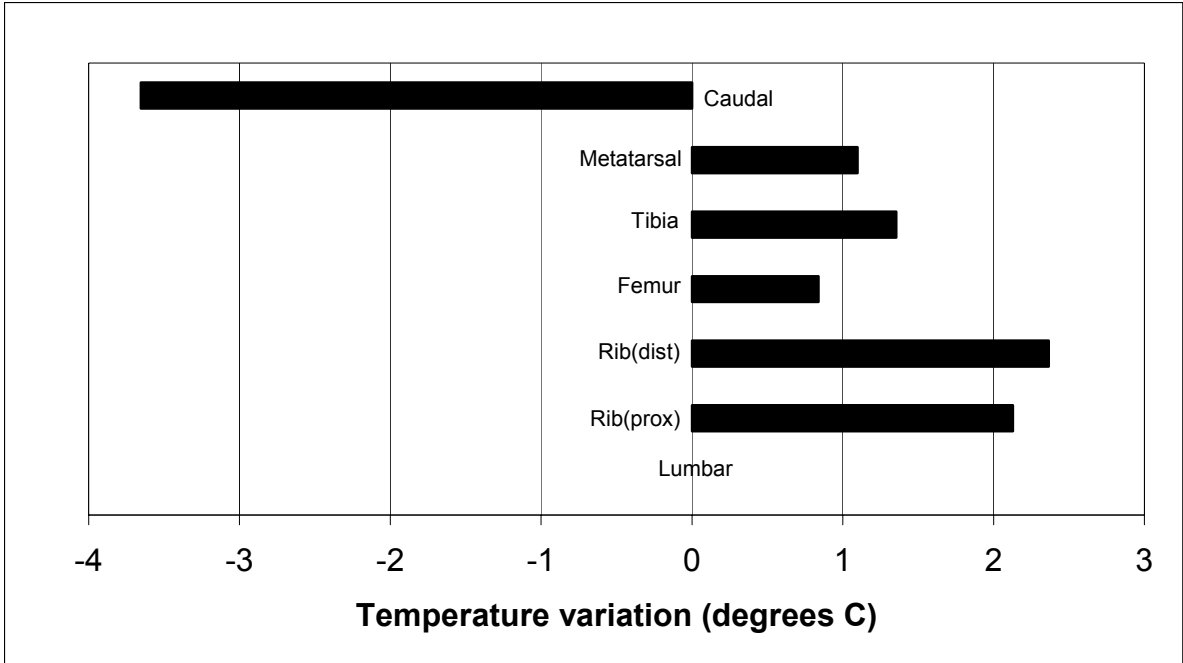


Figure 1.12 - Elephant interbone variation from the core body.

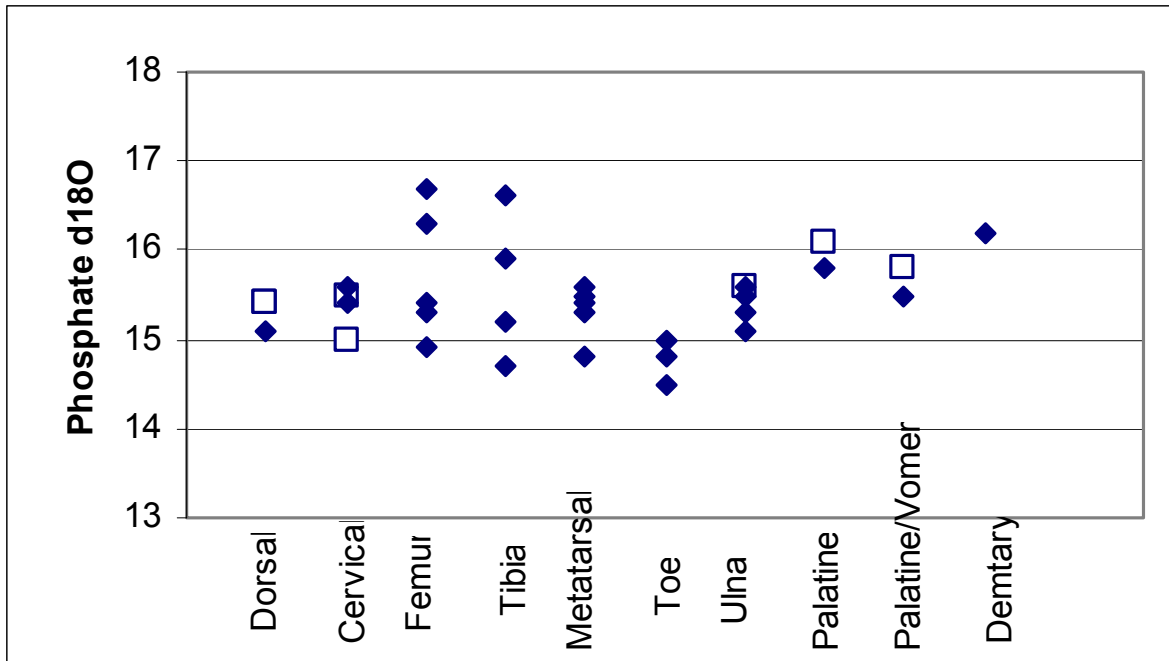


Figure 1.13 - Ostrich phosphate $\delta^{18}\text{O}$ values for each bone. All values are reported in permil units relative to V-SMOW. Closed diamonds represent compact bone; open squares represent spongy bone.

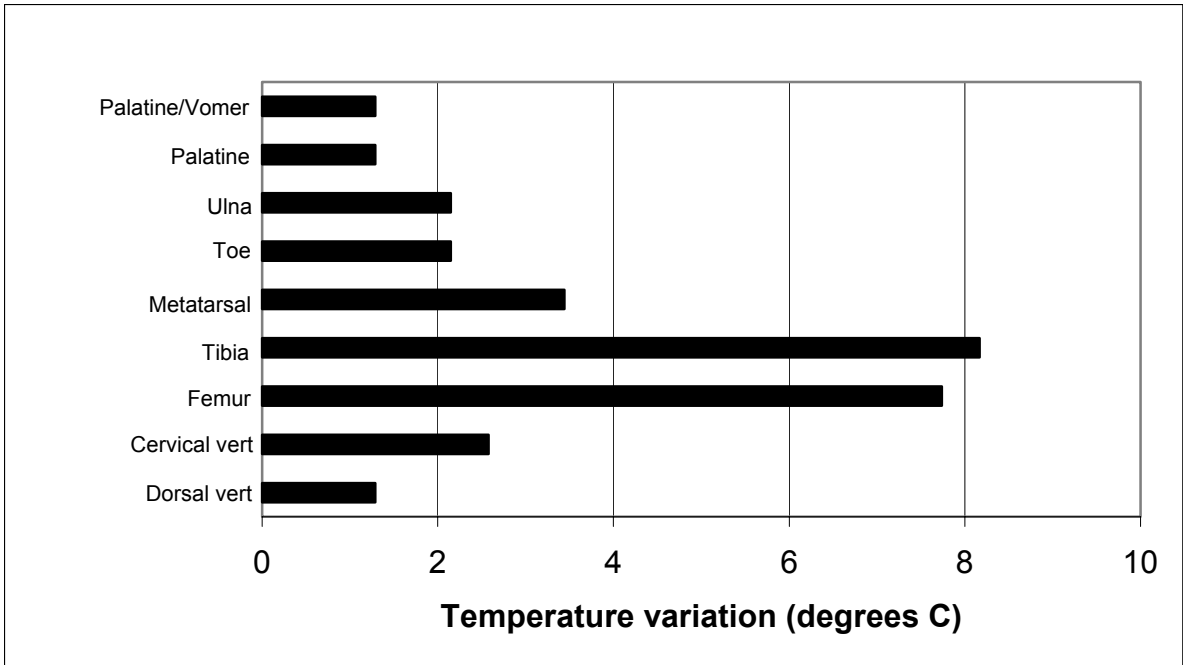


Figure 1.14 - Ostrich intrabone temperature variation for each bone.

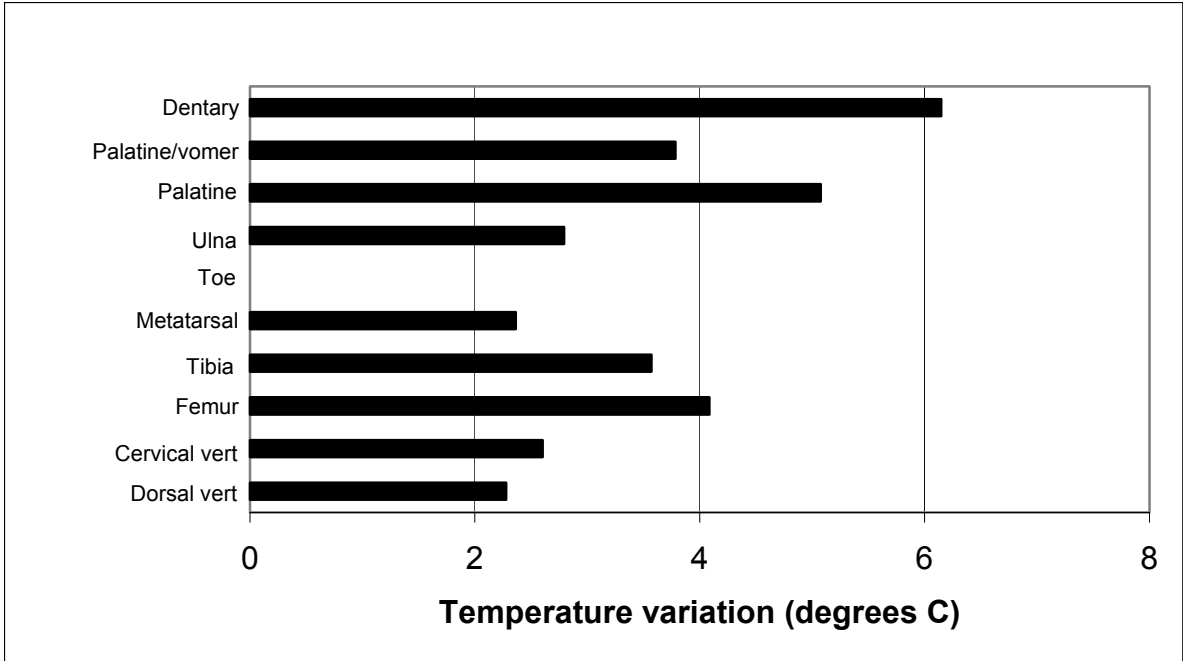


Figure 1.15 - Ostrich interbone temperature variation based on the warmest bone in the body.

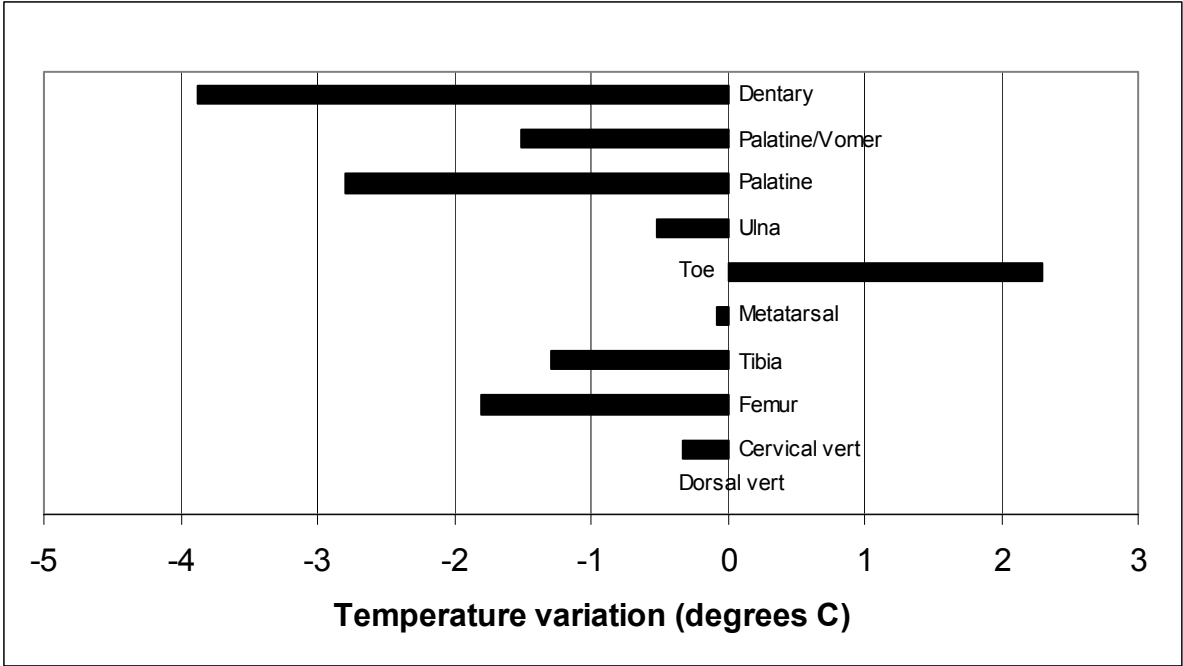


Figure 1.16 - Ostrich interbone temperature variation from the core body.

Chapter 2 – Examination of *Acrocanthosaurus atokensis*

Sample NCSM 14345 (*Acrocanthosaurus atokensis*) is here examined in an effort to determine thermoregulatory functions and adaptations.

MATERIALS AND METHODS

The bones of NCSM 14345 were drilled in a similar fashion to the modern bones. Approximately 30-50mg of powder was drilled from various sites on each bone using a common rotary tool with an engraving bit. Bones were selected according to availability and quality of preservation. From the preserved bones, sample sites were selected to cover all the major body regions (i.e. core body, limbs, tail, head) in order to provide a wide array of interbone temperature comparisons. Long bones were drilled at multiple sites to provide a progressive display of temperature variation between the proximal and distal body regions. Each site consisted of several depths encompassing cancellous and compact bone to provide intrabone temperature variations. The bone powders were then processed for phosphate and carbonate isotope analysis according to the procedures outlined in the following sections.

Phosphate oxygen isotopes:

Bone phosphate was isolated from all modern material according to procedures described in Dettman et al. (2001). Approximately 5-10mg of sample powder was

reacted overnight at room temperature in 1mL of 2M hydrofluoric acid. Four mL of deionized water was added, the mixture centrifuged, and the supernatant saved. The supernatant from a second 5mL rinse of the residual powder was added to the first. The resulting 10mL of supernatant was buffered with 0.8mL of 20% ammonium hydroxide solution. One mL of 2M silver nitrate solution was added and the resulting silver phosphate precipitate was washed with three separate deionized water rinses where the supernatant after centrifuging was discarded. The remaining solid was dried for two days at $\sim 100^{\circ}\text{C}$.

Approximately 500 μg of silver phosphate powder was loaded into a small combustible silver boat for each sample (3.5 x 5 mm, Costech, Valencia, CA). The samples were then analyzed using a Thermo Finnigan (Brennan, Germany) DELTA^{plus}XL dual inlet/continuous flow isotope ratio mass spectrometer coupled to a Thermo Finnigan TC/EA (thermo-chemical elemental analyzer). At a reaction temperature of 1450 $^{\circ}\text{C}$ in contact with glassy carbon, the oxygen in the silver phosphate is converted to carbon monoxide. The resulting gases from the combustion reaction, including the CO, are separated in a gas chromatograph column of 5A mole sieve held at 85 $^{\circ}\text{C}$. Once separated, the CO is admitted to the isotope ratio mass spectrometer and referenced against an internal reference CO gas (Messer, Duisberg, Germany; $-5.5 \pm 2.0\text{‰}$ $\delta^{18}\text{O}$ vs V-SMOW) admitted through the dual inlet bellow. Raw data are normalized using sucrose ANU (NBS RM 8542), an internal sucrose standard, and three internal silver phosphate standards of known value, previously normalized against NBS-

127 barium sulfate (NBS RM 8557) and sucrose ANU. Isotopic values are reported relative to V-SMOW in the standard δ notation where $\delta^{18}\text{O} = [(R_{\text{sample}}/R_{\text{standard}}) - 1] * 1000$ and $R = {}^{18}\text{O}/{}^{16}\text{O}$.

Carbonate oxygen and carbon isotopes:

Bone carbonate was isolated from all modern material according to a modification of the procedures of Bryant et al. (1996). Approximately 5mg of sample powder was reacted overnight in a 2-3% sodium hypochlorite solution at room temperature to remove any organic carbon compounds. The remaining powder was rinsed three times with deionized water and dried for two days at $\sim 100^\circ\text{C}$.

All $\delta^{18}\text{O}$ and $\delta^{13}\text{C}$ values of the dried powder were measured on a Micromass (Manchester, UK) dual inlet/continuous flow isotope ratio mass spectrometer coupled to a Micromass Multiprep carbonate analysis apparatus. Approximately 500-800 μg of powder was reacted with 100% phosphoric acid at 90°C in a vial under high vacuum. An aliquot of the released CO_2 was then injected into the mass spectrometer through a Gilson needle autosampler, cryogenically purified in a liquid nitrogen trap, and referenced against an internal CO_2 gas admitted via the dual inlet bellow in the mass spectrometer.

Oxygen isotopic values are reported relative to V-SMOW in the standard δ notation. $\delta^{18}\text{O} = [(R_{\text{sample}}/R_{\text{standard}}) - 1] * 1000$ where $R = {}^{18}\text{O}/{}^{16}\text{O}$. Carbon isotopic values are relative to V-PDB. $\delta^{13}\text{C} = [(R_{\text{sample}}/R_{\text{standard}}) - 1] * 1000$ where $R = {}^{13}\text{C}/{}^{12}\text{C}$.

Standards:

The precision of $\delta^{18}\text{O}$ values from phosphates was monitored by four standards. A wet chemistry laboratory standard (NAP) produced from 0.1M $\text{Na}_2\text{HPO}_4 \cdot 7\text{H}_2\text{O}$ solution was processed through the same procedure as the bone samples. The resulting precipitate yielded $\delta^{18}\text{O}$ values ± 0.13 permil (1σ). The mass spectrometry laboratory also used three in-house standards. AASP is an Alpha Aldrich (Ward Hill, MA) phosphate standard yielding $\delta^{18}\text{O}$ values ± 0.23 permil (1σ). SASP is an Alpha Aesar (Milwaukee, WI) phosphate standard yielding $\delta^{18}\text{O}$ values ± 0.24 permil (1σ). Finally, a laboratory sucrose standard yielded $\delta^{18}\text{O}$ values ± 0.25 permil (1σ).

Precision of $\delta^{18}\text{O}$ and $\delta^{13}\text{C}$ values from the carbonates was monitored by the house standard LL1. This is a pure carbonate rock from the Lincoln Limestone that has been calibrated with instrumentation at Harvard University to NBS-19, a NIST standard originally calibrated to the Peedee Belemnite (PDB). The LL1 standard yielded $\delta^{13}\text{C}$ values ± 0.052 permil (1σ) and $\delta^{18}\text{O}$ values ± 0.095 permil (1σ).

RESULTS AND DISCUSSION

Diagenesis:

An examination of post mortem diagenesis is necessary to determine the presence or absence of an original isotopic signature within the *Acrocanthosaurus* bones.

According to Iacumin et al. (1996) and Bryant et al. (1996), a comparison of the $\delta^{18}\text{O}_{\text{phosphate}}$ versus the $\delta^{18}\text{O}_{\text{carbonate}}$ should show little variation in the phosphate values relative to the carbonate values under circumstances where little or no diagenetic alteration has affected the phosphate. Due to the fact that phosphate ions hold more tightly to their oxygen atoms than do carbonate ions, one would expect the carbonate $\delta^{18}\text{O}$ values to have a greater variation as a result of groundwater resetting the isotopic ratios. However, Luz and Kolodny (1991) argue the opposite scenario where a linear correlation is in fact indicative of diagenetic alteration. The data presented in Fig. 2.1 show little or no correlation between the carbonate and phosphate values ($r = -0.288$) of the *Acrocanthosaurus atokensis*. The phosphates show a range of 3.0‰ and the carbonates a range of 4.0‰. The variance of the $\delta^{18}\text{O}_{\text{phosphate}}$ values is lower than that of the $\delta^{18}\text{O}_{\text{carbonate}}$ values ($p < 0.01$). The pattern appears to mimic that seen in the modern unaltered specimens and Luz and Kolodny (1991). Contrary to Iacumin et al. (1996), the modern specimens in this study suggest that diagenesis resetting the phosphate values would reset the carbonates as well, thereby creating a direct correlation between

$\delta^{18}\text{O}_{\text{phosphate}}$ and $\delta^{18}\text{O}_{\text{carbonate}}$ values. The absence of this correlation in the fossil suggests that the bone phosphates retain their original isotopic signature.

In conjunction with the phosphate versus carbonate comparisons, it is necessary to examine the standard deviations of said values associated with the two bone types. Compact bone is denser than cancellous bone, is less susceptible to groundwater infiltration, and has less exposed surface area for chemical reaction per volume. It can therefore be expected to show a lower variation among its $\delta^{18}\text{O}_{\text{phosphate}}$ values than cancellous bone if diagenesis has in fact altered the bone values. The data represented by Fig. 2.2 show an approximately equal standard deviation for the compact bone data as compared to the cancellous data. Statistical analysis (F-test with $n_1=37$, $n_2=28$, $\alpha=0.05$) suggests that the two values are similar ($p > 0.1$). Given the lack of correlation between $\delta^{18}\text{O}_{\text{phosphate}}$ and $\delta^{18}\text{O}_{\text{carbonate}}$ values this similarity provides further evidence that the bones have retained an original isotopic signature in the phosphates.

Results and discussion from the previous chapter suggest that these methods of examining diagenesis may not be entirely sufficient. However, a comparison of the bone $\delta^{18}\text{O}_{\text{phosphate}}$ and $\delta^{18}\text{O}_{\text{carbonate}}$ values from the infilling carbonate cements provides further evidence regarding diagenesis. The data suggest that these two values are significantly different ($p < 0.001$). Therefore, the groundwater that resulted in carbonate cement deposition did not affect or reset the phosphate oxygen values of the bones. Fig. 2.3 shows a much greater range in values for the carbonate cements compared to the

phosphate. The variance of the $\delta^{18}\text{O}_{\text{phosphate}}$ from the bone is lower than that of the $\delta^{18}\text{O}_{\text{carbonate}}$ from the infilling cement ($p = 0.01-0.025$). As previously mentioned, if both the carbonate and the phosphate exhibit near-equilibrium values with similar ranges, diagenetic alteration of isotopic signals might be indicated. This pattern is not seen in the data, therefore the *Acrocantosaur* specimen is assumed to yield an original isotopic signature.

Criticism of using oxygen isotope values from fossil bones to examine diagenesis has focused mostly on the potential over-printing of original isotopic signatures by diagenetic signals (Kolodny et al. 1996). The fossilization process often includes the recrystallization of biologic apatite to carbonate-fluor apatite, a process which is suggested as a potential source of fractionation and an alteration pathway of original isotopic signatures to diagenetic values. This process is usually accompanied by the inclusion of relatively high concentrations of rare earth elements (REEs) in the secondary crystals. However, isotopic exchange between oxygen in water and oxygen in phosphate is extremely slow in inorganic reactions (Tudge 1960). Therefore recrystallization should not produce a significant fractionation in inorganic reactions where the phosphate ions do not dissociate. X-ray diffraction analyses can determine the percents of biologic apatite and carbonate-fluor apatite in a specimen, thus quantifying the degree (or lack thereof) of recrystallization. In-situ laser ablation techniques might then be able to focus isotopic analyses on individual crystals, thereby providing a method to determine the isotopic differences between original and secondary phosphates in fossil bone. While these

procedures are beyond the scope of this project, they represent valuable avenues for future research. At present the previously discussed data is considered adequate evidence that the *Acrocanthosaurus* bone phosphate retains original isotopic signatures.

Examination of thermoregulation:

The range of $\delta^{18}\text{O}_{\text{phosphate}}$ values varies markedly between the different bones (Fig. 2.4). The ulna exhibits the greatest range while the distal hole of the sacral spine exhibits the least. These differences manifest themselves in different intrabone temperature variations (Fig. 2.5). The ulna shows $\sim 7.7^\circ\text{C}$ change within itself while the sacral spine shows only $\sim 1.1^\circ\text{C}$. Interestingly, several of the core body bones exhibit temperature variations equal to that of the outer extremities.

A comparison of the temperature variation between bones shows a dramatic anomaly in the braincase (Fig. 2.4 and 2.6). This bone appears much warmer than any other bone in the body. The remaining bones vary more from the braincase alone than they do from one another. Of specific note are the drastic differences between the bones of the head. The palatal and the braincase differ by almost 9°C . *Acrocanthosaurus* appears to have had need of some physiological mechanism that kept the brain at a higher temperature than the rest of the body.

A comparison of interbone temperature variation using the dorsal rib as a zero point suggests that all the bones except the braincase stayed within the $\pm 4^\circ\text{C}$ bounds of homeothermy (Fig. 2.7). It appears that bones close to one another show similar

variations from the core body (i.e. the tibia and femur or the two holes on the sacral spines). However, the distal bones show a slightly warmer temperature than the more proximal ones. Specifically, the metatarsal is 1°C warmer than the femur. This could be a size-related issue considering that the data showed a similar phenomenon in the elephant (Chapter 1). The pattern also mimics that of the ostrich where a distal foot bone exhibits warmer temperatures due to contact with a hot substrate. Given the *Acrocanthosaurus*'s digitigrade posture, this scenario is plausible. Some of the more distal bones show cooler temperatures than the core body. Specifically, the caudal and the ulna are 3.1°C and 1.1°C cooler, respectively. For both these bones the observed pattern is most likely due to their distance from the core body and relative lack of insulation.

Various points on the sacral spines showed temperatures at a maximum of 2.2°C warmer than the dorsal rib. While this difference is slight, it is significant ($p = 0.1-0.05$). The spines may have served as a heat-shedding mechanism similar to that of the alligator palate where warm blood is shunted to the structure in an effort to cool it by way of convection. This process manifests itself in warmer temperatures during bone deposition for the *Acrocanthosaurus* spines or the alligator palate versus the core body bones. Interestingly, the palatal and vomer of the *Acrocanthosaurus* are cooler than the core body. This suggests that the animal was not shunting warm blood to that area. However, it may still have opened its mouth and used the palate as a heat-exchange surface thereby producing cooler temperatures through an evaporative effect in that region than in the

core body. The pterygoid, which is near both of the aforementioned palate bones, appears warmer than the core body and the palate. Given its proximity to the extremely warm braincase, it is likely that the latter affected the temperature of the pterygoid.

A comparison with the modern animals suggests that *Acrocanthosaurus* most resembles a homeothermic endotherm in its patterns of temperature variation. The intrabone temperature variation most closely resembles the elephant and the ostrich (Fig. 2.5, 1.12, and 1.16). The interbone temperature variation does not directly mimic any of the modern animals, but it appears as a mix of the elephant and the ostrich (Fig. 2.7, 1.14, and 1.18). A comparison of ranges in the $\delta^{18}\text{O}_{\text{phosphate}}$ values between all the animals suggests an *Acrocanthosaurus* pattern similar to that of the endothermic ostrich and elephant (Fig. 2.8). The femur shows more temperature variation than either the foot bones or the core body, while the latter show a close similarity to one another. It is notable that the *Acrocanthosaurus* pattern observed in Figure 2.8 does not conform precisely to any of the modern analogues. It appears as an intermediate between the ectotherm and the two endotherms with a closer resemblance to the latter. The actual temperature variation within the *Acrocanthosaurus* is slightly higher than the ostrich and elephant, yet still within the bounds of homeothermy. Statistical comparison of the *Acrocanthosaurus* $\delta^{18}\text{O}_{\text{phosphate}}$ values from the body show standard deviations similar to those of the ostrich and elephant bodies ($p > 0.2$). However, *Acrocanthosaurus* shows a statistically lower deviation than the alligator ($p = 0.05-0.10$).

The pattern appears to resemble a regional heterotherm or it could suggest some intermediate form of homeothermic endothermy. Homeothermic ectothermy is a possibility, although it seems unlikely as the *Acrocanthosaurus* bears little resemblance to the alligator patterns. The distinction between endotherm versus ectotherm is one that can not be clearly determined based on these data alone. *Acrocanthosaurus* may have maintained a constant body temperature due to the fact that it lived in a warm environment rather than actual metabolic heat production (i.e. endothermy). However, this scenario is refuted by the evidence suggesting at least some heat-shedding mechanisms on the body. Additionally, the ability to maintain brain temperatures above those exhibited by other skeletal elements argues against an ectothermic physiology.

Explaining the anomalous braincase presents an interesting difficulty. Evidence from ectothermic animals suggests that brain temperatures are usually kept below the body temperature by countercurrent exchange systems if any regulation exists at all (Johnson 1972, Crawford et al. 1977, Dodson 1977, Bartholemew 1982). Endotherms often exhibit higher brain versus body temperatures even if they have the ability to control brain temperature through the use of complex nested cranial blood vessels known as carotid retes (Block and Carey 1985, Mitchell et al. 2002). This tentatively suggests that *Acrocanthosaurus* follows a more endothermic pattern of temperature distribution. However, endotherms that have produced this pattern in past studies are often mammalian or aquatic. This comparison might then be inaccurate for a clearly terrestrial dinosaur. It cannot currently be determined from the bones alone if *Acrocanthosaurus*

had any such blood vessel pattern that could serve as a countercurrent system to keep the brain either cool or warm.

Amongst the terrestrial animals, an ectothermic heterotherm attempting to warm its brain relative to its body generally uses environmental heat to do so. It seems unlikely that an animal the size of *Acrocanthosaurus* could continually hide its body in shade or a burrow to prevent heat gain in the body while exposing the head to the sun. It is more likely that the high brain temperature was due to active metabolic control of the brain/body temperature differential. Given that there is evidence of heat shedding mechanisms on the *Acrocanthosaurus* body, it is probable that the body itself was kept at a temperature below that of the core body. The brain was then at the core body temperature or slightly above it. A preserved dorsal centrum would provide a better proxy for the core body temperature than the ribs. The ribs are covered by less flesh than a dorsal centrum and may therefore be at a slightly lower temperature. Until a more complete specimen is found, the precise difference between the brain and core body can not be quantified. Regardless, the temperature difference exhibited between the ribs and the brain suggests an active metabolic strategy.

An explanation might be found in the behavior or the life history of *Acrocanthosaurus*. Body morphology suggests that it was definitely a predator. Nocturnal predation would possibly require metabolic heat to warm the brain while the rest of the body lost heat in the cooler night temperatures. Diurnal hours were then spent with less activity and shedding heat. Another possibility is variation in bone remodeling

rates. Braincase bone tends to remodel more slowly than other skeletal elements and therefore records a different life stage. A highly active metabolism and subsequent heat production during juvenile growth would be recorded by all the bones, but most would lose that original signature upon reaching adult status. It is possible that in its lifetime, *Acrocanthosaurus* experienced a drastic change in the isotopic values of its drinking water. While NCSM 14345 has been classified as an adult, its precise age is unknown. The rate of braincase bone remodeling in dinosaurs and the time induced changes in environmental water isotopic values are also currently unknown. Future study of these issues would present valuable evidence for this case study. A third possibility is the mode of death for this particular individual. No suggestions have been made, but disease and extreme fever are an option. However, it is necessary to know the minimal duration of time the fever would need to exist in order for the heightened temperature to be recorded by the bones. Future study of modern animal fever duration versus bone deposition rate during a time of sickness could clarify the issue.

The dramatic difference between the head and body temperature allows for broad climate interpretation and placement of this specimen within the rise of the Cretaceous hot-house environment. As the actual brain temperature is unknown, an assumption can be made based on the current indications that *Acrocanthosaurus* had a more endothermic homeothermic strategy. The average brain temperature for endotherms is $\sim 37\text{-}38^{\circ}\text{C}$ (Donhoffer 1980). With a difference of $\sim 8^{\circ}\text{C}$ between the ribs and the brain, it follows that the core body was $\sim 29\text{-}30^{\circ}\text{C}$. Some of the bones are slightly cooler than the core

indicating that the environmental temperature was even lower – perhaps approximately 24-27°C. This temperature estimate is in the middle range of temperatures suggested by paleoclimate research for the entire Cretaceous period (Fassell and Bralower 1999, Frakes 1999, Sellwood et al. 1994). Even when one incorporates several degrees of error due to the assumptions made in this calculation, the temperature estimate still falls within previously established Cretaceous temperatures. It appears that *Acrocanthosaurus* existed during the rise of the Cretaceous temperatures prior to the maximum of the hot-house environment. While these temperature estimates require further research to support them, the suggestion still remains that this animal did not maintain a constant body temperature due to consistently high environmental temperatures. The implications for an endothermic homeothermic metabolism are sustained.

CONCLUSIONS

Analyses of $\delta^{18}\text{O}_{\text{carbonate}}$ and $\delta^{18}\text{O}_{\text{phosphate}}$ values suggest that the *Acrocanthosaurus* specimen has retained an original isotopic signature in the bone phosphate. This signature follows the endothermic homeothermic pattern of the modern elephant and ostrich more closely than it does the modern alligator. Heat shedding mechanisms, high brain temperatures, and a predatory life style suggest an active metabolism. In the context of the overall Cretaceous environment, this *Acrocanthosaurus* was maintaining a fairly constant body temperature in an environment that was moving towards a hot-house climate.

FUTURE WORK

While several methods can be used to examine the diagenesis of a fossil specimen, the one in greatest contention concerns the correlation between $\delta^{18}\text{O}_{\text{phosphate}}$ and $\delta^{18}\text{O}_{\text{carbonate}}$ values. This correlation (or lack thereof) is best resolved by extensive analysis of modern animals. Thermographic scans and insertion of temperature diodes in live animals could determine which of the two ions is the better indicator of actual body temperature. Additional examination of overprinting can be performed using the previously suggested analyses of recrystallization and REE presence.

Observations from the *Acrocanthosaurus atokensis* specimen would be considerably strengthened by similar studies on other *A. atokensis* individuals. Considering that this is currently a rare species, analyses of closely related genera such as *Giganotosaurus* and *Charcharodontosaurus*, or the slightly more distantly related *Tyrannosaurus* and *Allosaurus* might suffice. More cranial data is necessary to discern if the anomalous braincase of the *Acrocanthosaurus* is a common trend or a unique situation. The aforementioned determination of actual body temperatures would also serve to strengthen conclusions about the actual thermoregulatory functioning of this dinosaur.

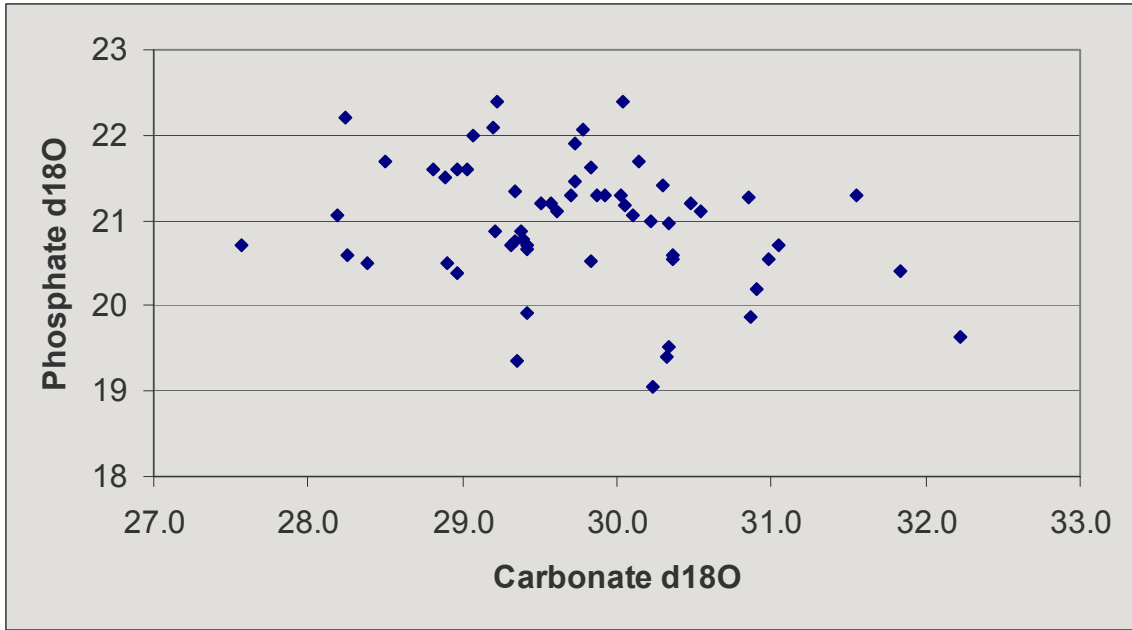


Figure 1.1 - *Acrocanthosaurus* phosphate $\delta^{18}\text{O}$ versus carbonate $\delta^{18}\text{O}$ values. All values are reported in permil units relative to V-SMOW.

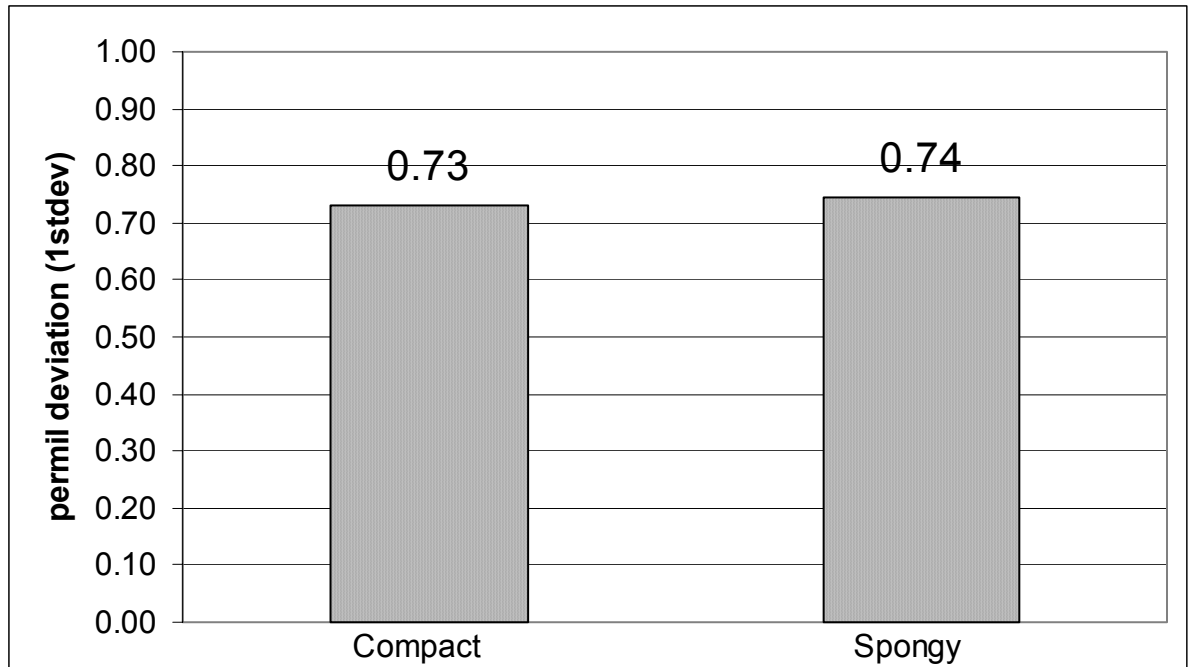


Figure 2.2 - Standard deviation of collected *Acrocanthosaurus* data for each bone type. Printed values represent one standard deviation from the mean.

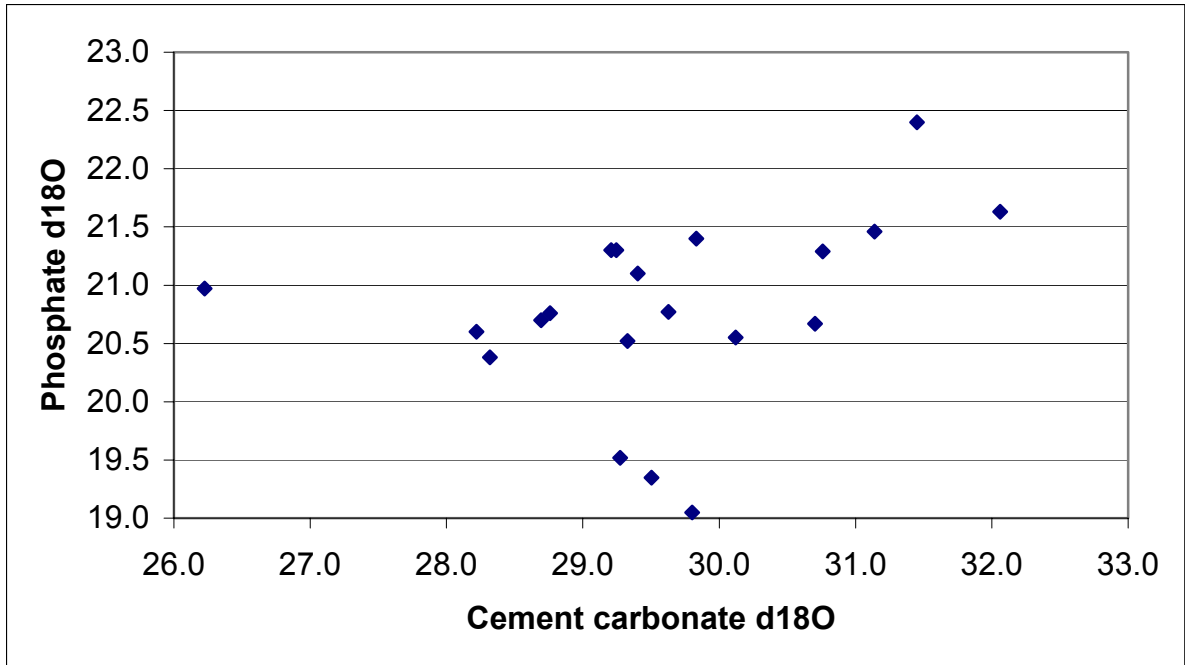


Figure 2.3 - *Acrocanthosaurus* phosphate $\delta^{18}\text{O}$ versus carbonate cement $\delta^{18}\text{O}$ values. All values are reported in permil units relative to V-SMOW.

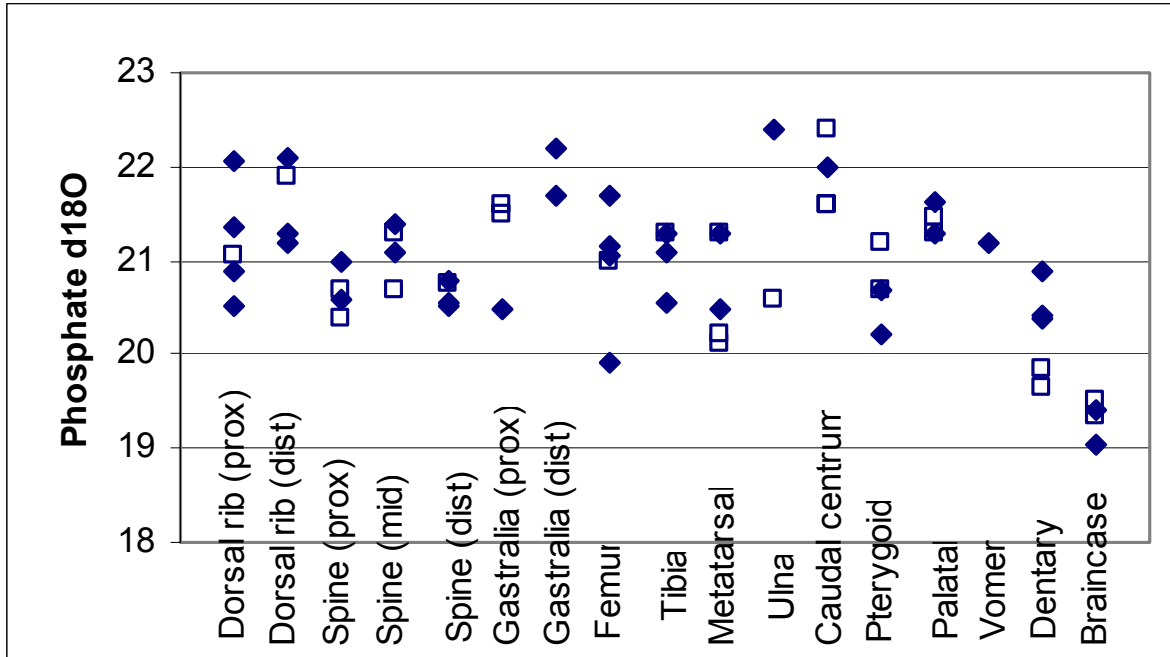


Figure 2.4 - *Acrocanthosaurus* phosphate $\delta^{18}\text{O}$ values for each bone. All values are reported in permil units relative to V-SMOW. Closed diamonds represent compact bone; open squares represent spongy bone.

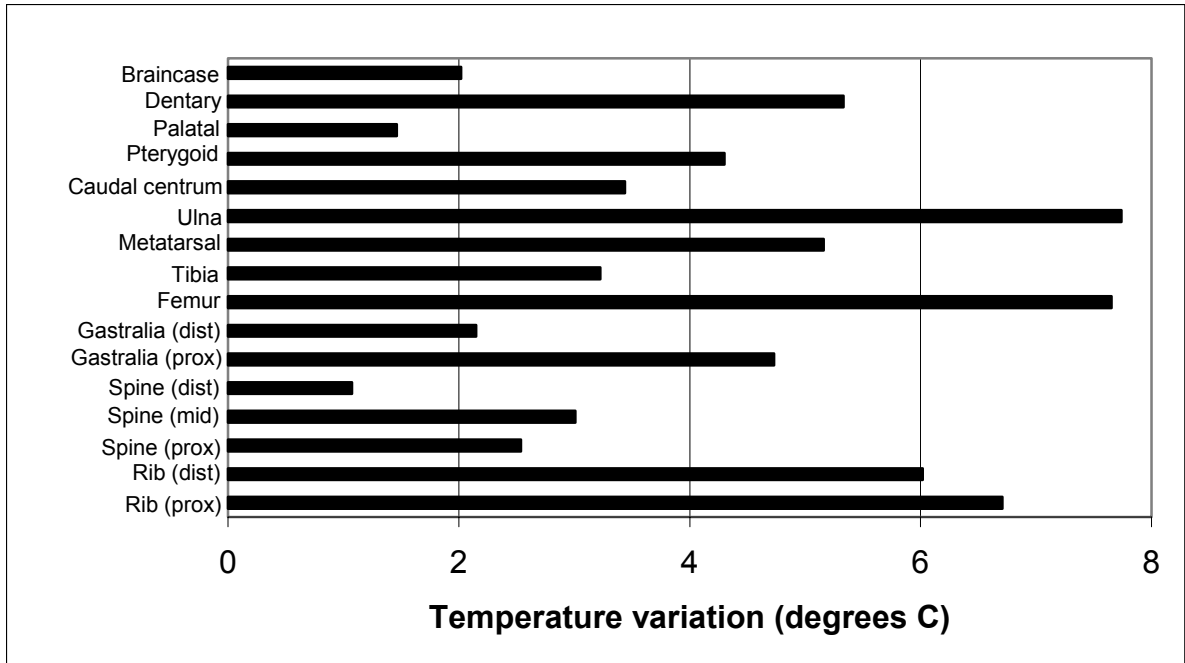


Figure 2.5 - *Acrocanthosaurus* intrabone temperature variation for each bone.

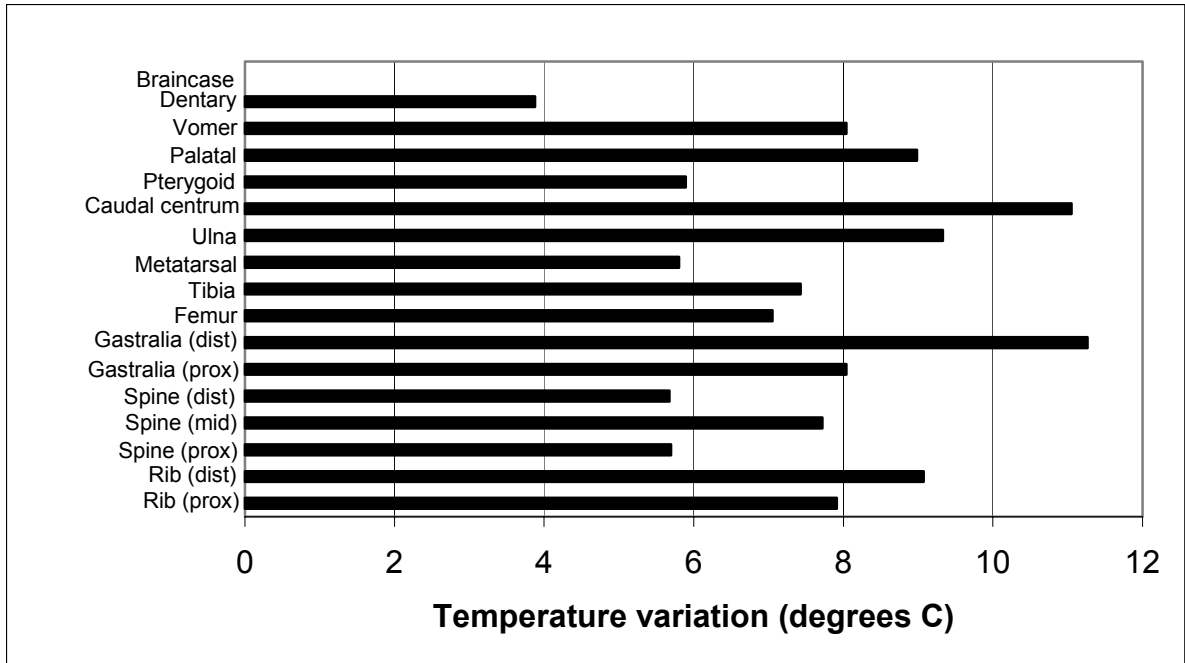


Figure 2.6 - *Acrocanthosaurus* interbone temperature variation based on the warmest bone in the body.

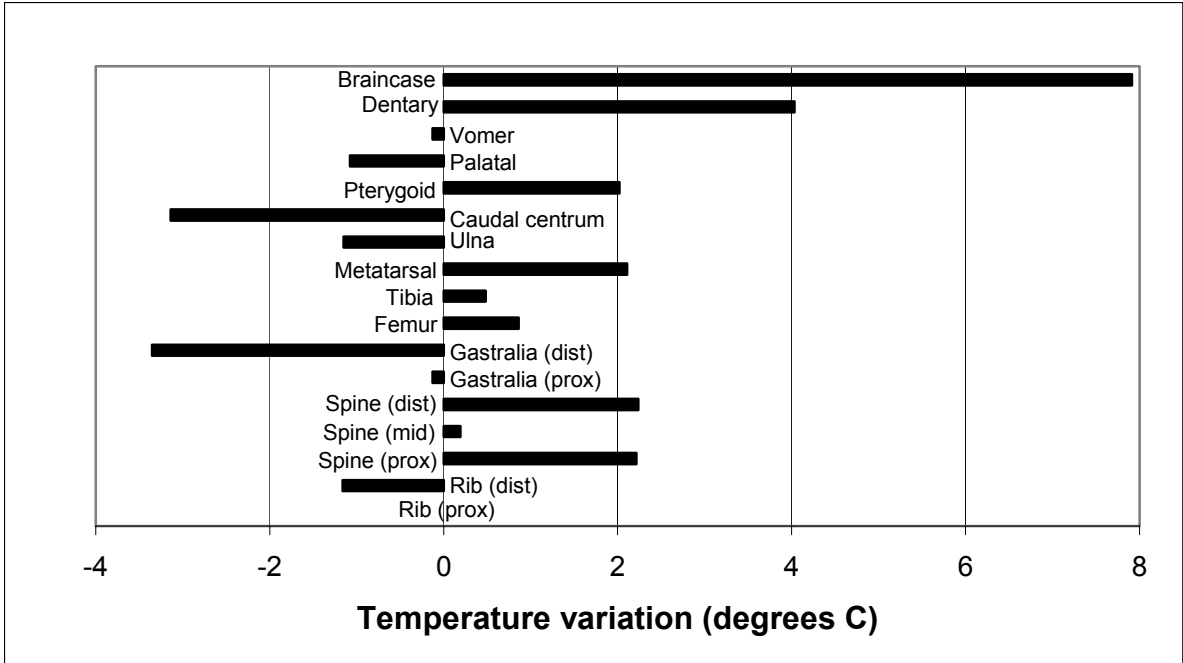


Figure 2.7 - *Acrocanthosaurus* interbone temperature variation from the core body.

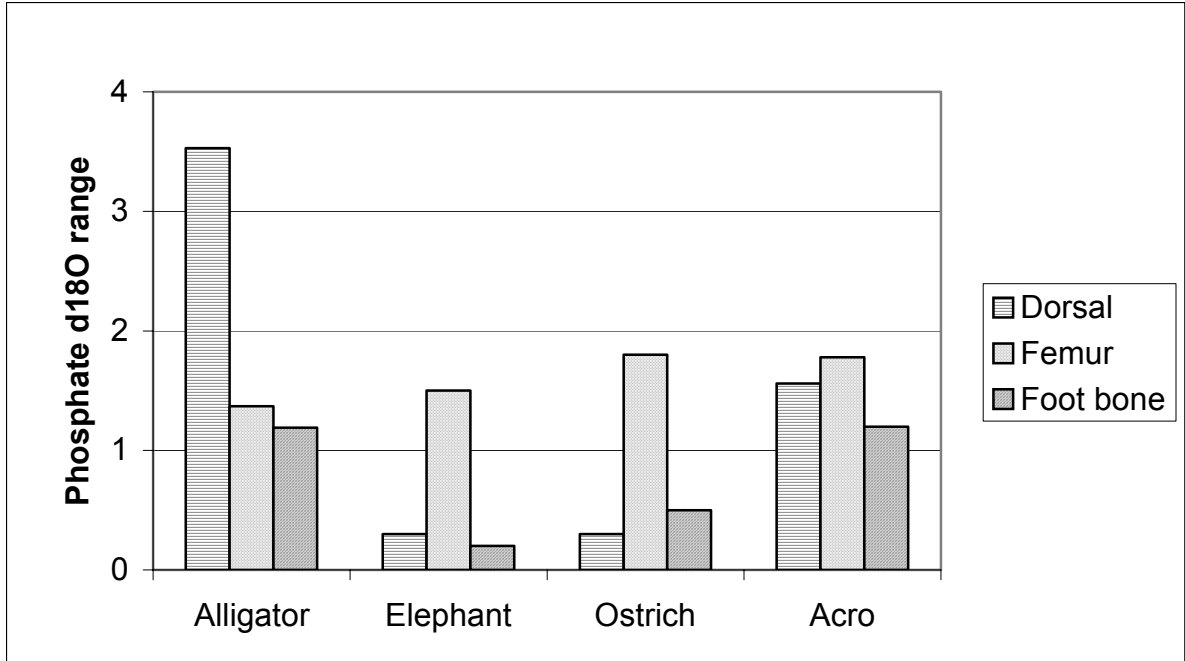


Figure 2.8 - Range of phosphate $\delta^{18}\text{O}$ values for the core, mid, and distal regions of the body. Ranges are reported as a permil difference.

References

- Barrick, R.E., and Kohn, M.J., 2001. Multiple taxon – multiple locality approach to providing oxygen isotope evidence for warm-blooded theropod dinosaurs: comment and reply. *Geology*: 565-566.
- Barrick, R.E., and Showers, W.J., 1994. Thermophysiology of *Tyrannosaurus rex*: evidence from oxygen isotopes. *Science* 265: 222-224.
- Barrick, R.E., and Showers, W.J., 1995. Oxygen isotope variability in juvenile dinosaurs (*Hypacrosaurus*): evidence for thermoregulation. *Paleobiology* 21(4): 552-560.
- Barrick, R.E., and Showers, W.J., 1999. Thermophysiology and biology of *Giganotosaurus*: Comparison with *Tyrannosaurus*. *Palaeontologia Electronica*: http://www-odp.tamu.edu/paleo/1999_2/gigan
- Barrick, R.E., Fischer, A.G., and Showers, W.J., 1999. Oxygen isotopes form turtle bone: applications for terrestrial paleoclimates? *Palaios* 14: 186-191.
- Barrick, R.E., Stoskopf, M.J., Marcot, J.D., Russell, D.A., and Showers, W.J., 1998. The thermoregulatory functions of the *Triceratops* frill and horns: heat flow measured with oxygen isotopes. *Journal of Vertebrate Paleontology* 18(4): 746-750.
- Barrick, R.E., Showers, W.J., and Fischer, A.G., 1996. Comparison of thermoregulation of four ornithischian dinosaurs and a varanid lizard from the Cretaceous Two Medicine Formation: evidence form oxygen isotopes. *Palaios* 11: 295-305.
- Barron, E.J., 1983. A warm, equable Cretaceous: the nature of the problem. *Earth Science Reviews* 19: 305-338.
- Bartholomew, G.A., 1982. Physiological Control of Body Temperature. In: Gans, C., and Pough, F.H., eds. *Biology of the Reptilia*, vol.12. Academic Press, London.
- Bligh, J., and Johnson, K.G., 1973. Glossary for terms for thermal physiology. *Journal of Applied Physiology* 35(6): 941-961.
- Block, B.A., and Carey, F.G., 1985. Warm brain and eye temperatures in sharks. *Journal of Comparative Physiology B* 156: 229-236.
- Brainerd, E.L., 1999. New perspectives on the evolution of lung ventilation mechanisms in vertebrates. *Experimental Biology* 4(2): 11-28.
- Brochu, C.A., 2003. Osteology of *Tyrannosaurus rex*: insights from a nearly complete skeleton on high-resolution computed tomographic analysis of the skull. *Journal of Vertebrate Paleontology* 22 (supplement to 4): 1-138.
- Bryant, J.D., Koch, P.L., Froelich, P.N., Showers, W.J., and Genna, B.J., 1996. Oxygen isotope partitioning between phosphate and carbonate in mammalian apatite. *Geochimica et Cosmochimica Acta* 60(24): 5145-5148.
- Crawford, E.C. Jr., Palomeque, J., and Barber, B.J., 1977. A physiological basis for head body temperature differences in a panting lizard. *Comparative Biochemistry and Physiology* 56A: 161-163.

- Currie, P.J., and Carpenter, K., 2000. A new specimen of *Acrocanthosaurus atokensis* (Theropoda, Dinosauria) from the Lower Cretaceous Antlers Formation (Lower Cretaceous, Aptian) of Oklahoma, USA. *Geodiversitas* 22(2): 207-246.
- D'Angela, D., and Longinelli, A., 1990. Oxygen isotopes in living mammal's bone phosphate: further results. *Chemical Geology* 86: 75-82.
- Davis, J.E., Spotila, J.R., and Scheffler, W.C., 1980. Evaporative water loss from the American alligator, *Alligator mississippiensis*: the relative importance of respiratory and cutaneous components and the regulatory role of the skin. *Comparative Biochemistry and Physiology* 67A: 439-446.
- Dawson, T.J., 1972. Thermoregulation in Australian desert kangaroos. *Symposia of the Zoological Society of London* 31: 133-146.
- Dettman, D.L., Kohn, M.J., Quade, J., Ryerson, F.J., Ojha, T.P., and Hamidullah, S., 2001. Seasonal stable isotope evidence for a strong Asian monsoon throughout the past 10.7 m.y. *Geology* 29(1): 31-34.
- Dodson, P., 1977. Mouth gaping as an affective thermoregulatory device in alligators. *Nature* 265: 235-236.
- Earll, C.R., 1982. Heating, cooling and oxygen consumption rates in *Varanus bengalensis*. *Comparative Biochemistry and Physiology* 72A (2): 377-381.
- Epstein, S., Buchsbaum, R., Lowenstam, H.A., and Urey, H.C., 1953. Revised carbonate-water isotopic temperature scale. *Bulletin of the Geological Society of America* 64: 1315-1326.
- Erickson, G.M., Rogers, K.C., and Yerby, S.A., 2001. Dinosaurian growth patterns and rapid avian growth rates. *Nature* 412: 429-432.
- Fassell, M.L., and Bralower, T.J., 1999. Warm, equable mid-Cretaceous: stable isotope evidence. In: Barrera, E., and Johnson, C.C., eds. *Evolution of the Cretaceous Ocean-Climate System*. Boulder, Colorado. Geological Society of America Special Paper 332.
- Fisher, P.E., Russell, D.A., Stoskopf, M.K., Barrick, R.E., Hammer, M., and Kuzmitz, A.A., 2000. Cardiovascular evidence for an intermediate or higher metabolic rate in an Ornithischian dinosaur. *Science* 288: 503-505.
- Frakes, L.A., 1999. Estimating the global thermal state from Cretaceous sea surface and continental temperature data. In: Barrera, E., and Johnson, C.C., eds. *Evolution of the Cretaceous Ocean-Climate System*. Boulder, Colorado. Geological Society of America Special Paper 332.
- Fricke, H.C., and O'Neil, J.R., 1996. Inter- and intra- tooth variation in the oxygen isotope composition of mammalian tooth enamel phosphate: implications for palaeoclimatological and palaeobiological research. *Palaeogeography, Palaeoclimatology, Palaeoecology* 126: 91-99.
- Fricke, H.C., and Rogers, R.R., 2000. Multiple taxon – multiple locality approach to providing oxygen isotope evidence for warm-blooded theropod dinosaurs. *Geology* 28: 799-802.

- Fricke, H.C., and Rogers, R.R., 2001. Multiple taxon – multiple locality approach to providing oxygen isotope evidence for warm-blooded theropod dinosaurs: comment and reply. *Geology*: 566-567.
- Haack, S.C., 1986. A thermal model of the sailback pelycosaur. *Paleobiology* 12(4): 450-458.
- Harris, J.D., 1998. A reanalysis of *Acrocanthosaurus atokensis*, its phylogenetic status, and paleobiogeographic implications, based on a new specimen from Texas. *Bulletin of the New Mexico Museum of Natural History and Science* 13: i-75.
- Hobday, D.K., and McKalips, D.G., 1979. Nonmarine depositional environments and uranium exploration in Lower Cretaceous Antlers Formation, North Texas. *AAPG Bulletin* 63(5): 831.
- Horner, J.R., 1995. Morphology and function of the enclosed narial chambers of lambeosaurid dinosaurs. *Journal of Vertebrate Paleontology* 15(supplemental): 36A.
- Huber, B.T., Hodell, D.A., and Hamilton, C.P., 1995. Middle-Late Cretaceous climate of the southern high latitudes: stable isotope evidence for minimal equator-to-pole thermal gradients. *GSA Bulletin* 107(10): 1164-1191.
- Huber, B.T., Norris, R.D., and MacLeod, K.G., 2002. Deep-sea paleotemperature record of extreme warmth during the Cretaceous. *Geology* 30(2): 123-126.
- Huey, R.B., 1982. Temperature, physiology, and the ecology of reptiles. In: Gans, C., and Pough, F.H., eds. *Biology of the Reptilia*, vol.12. Academic Press, London.
- Huey, R.B., and Slatkin, M., 1976. Cost and benefit of lizard thermoregulation. *The Quarterly Review of Biology* 51(3): 363-384.
- Iacumin, P., Bocherens, H., Mariotti, A., and Longinelli, A., 1996. Oxygen isotope analyses of co-existing carbonate and phosphate in biogenic apatite: a way to monitor diagenetic alteration of bone phosphate? *Earth and Planetary Science Letters* 142: 1-6.
- Johnson, C.R., 1972. Head-body temperature differences in *Varanus gouldii* (Sauria: Varanidae). *Comparative Biochemistry and Physiology* 43A: 1025-1029.
- Koch, P.L., Tuross, N., and Fogel, M.L., 1997. The effects of sample treatment and diagenesis on the isotopic integrity of carbonate in biogenic hydroxylapatite. *Journal of Archaeological Science* 24: 417-429.
- Kohn, M.J., 1996. Predicting animal $\delta^{18}\text{O}$: accounting for diet and physiological adaptation. *Geochimica et Cosmochimica Acta* 60(23): 4811-4829.
- Kolodny, Y., Luz, B., and Navon, O., 1983. Oxygen isotope variations in phosphate of biogenic apatite, I. Fish bone apatite – rechecking the rules of the game. *Earth and Planetary Science Letters* 64: 398-404.
- Kolodny, Y., Luz, B., Sander, M., and Clemens, W.A., 1996. Dinosaur bones: fossils or pseudomorphs? The pitfalls of physiology reconstruction from apatitic fossils. *Palaeogeography, Palaeoclimatology, Palaeoecology* 126: 161-171.

- Longinelli, A., 1984. Oxygen isotopes in mammal bone phosphate: a new tool for paleohydrological and paleoclimatological research? *Geochimica et Cosmochimica Acta* 48: 385-390.
- Longinelli, A., and Nuti, S., 1973. Revised phosphate-water isotopic temperature scale. *Earth and Planetary Science Letters* 19: 373-376.
- Lauw, G.N., 1972. The role of advective fog in the water economy of certain Namib Desert animals. In: Maloiy, G.M.O., *ed.* *Comparative Physiology of Desert Animals – Symposia of the Zoological Society of London #31*. Academic Press, London.
- Luz, B., and Kolodny, Y., 1985. Oxygen isotope variations in phosphate of biogenic apatites, IV. Mammal teeth and bones. *Earth and Planetary Science Letters* 75: 29-36.
- Luz, B., and Kolodny, Y. 1991. Oxygen isotopes in phosphates of fossil fish – Devonian to recent. In: Taylor, H.P., Jr., O’Neil, J.R., and Kaplan, I.R., *eds.* *Stable Isotope Geochemistry: A Tribute to Samuel Epstein*. The Geochemical Society, Special Publication No. 3.
- Luz, B., Cormie, A.B., and Schwarcz, H.P., 1990. Oxygen isotope variations in phosphate of deer bones. *Geochimica et Cosmochimica Acta* 54: 1723-1728.
- Luz, B., Kolodny, Y., and Horowitz, M., 1984. Fractionation of oxygen isotopes between mammalian bone-phosphate and environmental drinking water. *Geochimica et Cosmochimica Acta* 48: 1689-1693.
- McNab, B.K., and Auffenberg, W., 1976. The effect of large body size on the temperature regulation of the komodo dragon, *Varanus komodoensis*. *Comparative Biochemistry and Physiology* 55A: 345-350.
- Michael, F.Y., 1972. Planktonic foraminifera from the Comanchean series (Cretaceous) of Texas. *Journal of Foraminiferal Research* 2(4): 200-220.
- Mitchell, D., Maloney, S.K., Jessen, C., Laburn, H.P., Kamerman, P.R., Mitchell, G., and Fuller, A., 2002. Adaptive heterothermy and selective brain cooling in arid-zone mammals. *Comparative Biochemistry and Physiology Part B* 131: 571-585.
- Nelson, B.K., De Niro, M.J., Schoeninger, M.J., DePaolo, D.J., and Hare, P.E., 1986. Effects of diagenesis on strontium, carbon, nitrogen, and oxygen concentration and isotopic composition of bone. *Geochimica et Cosmochimica Acta* 50: 1941-1949.
- O’Connor, M.P., and Dodson, P., 1999. Biophysical constraints on the thermal ecology of dinosaurs. *Paleobiology* 25(3): 341-368.
- Ostram, P.H., Zonneveld, J.P., and Robbins, L.L., 1994. Organic geochemistry of hard parts: assessment of isotopic variability and indigeneity. *Palaeogeography, Palaeoclimatology, Palaeoecology* 107: 201-212.
- Padian, K., deRicqles, A.J., and Horner, J.R., 2001. Dinosaurian growth rates and bird origins. *Nature* 412: 405-408.

- Paladino, F.V., O'Connor, M.P., and Spotila, J.R., 1990. Metabolism of leatherback turtles, gigantothermy, and thermoregulation of dinosaurs. *Nature* 344: 858-860.
- Paul, G.S., 1995. Can nasal turbinates be used to diagnose paleometabolics? *Journal of Vertebrate Paleontology* 15(supplemental): 48A.
- Paul, G.S., 1996. The status of respiratory turbinates in theropods. *Journal of Vertebrate Paleontology* 16(supplemental): 57A.
- Person, A., Bocherens, H., Mariotti, A., and Renard, M., 1996. Diagenetic evolution and experimental heating of bone phosphate. *Palaeogeography, Palaeoclimatology, Palaeoecology* 126: 135-149.
- Person, A., Bocherens, H., Saliege, J., Paris, F., Zeitoun, V., and Gerard, M., 1995. Early diagenetic evolution of bone phosphate: an X-ray diffractometry analysis. *Journal of Archaeological Science* 22: 211-221.
- Phillips, P.K., and Heath, J.E., 1992. Heat exchange by the pinna of the African elephant (*Loxodonta africana*). *Comparative Biochemistry and Physiology* 101A(4): 693-699.
- Phillips, P.K., and Heath, J.E., 1995. Dependency of surface temperature regulation on body size in terrestrial mammals. *Journal of Thermal Biology* 20(3): 281-289.
- Phillips, P.K., and Sanborn, A.F., 1994. An infrared, thermographic study of surface temperature in three ratites: ostrich, emu and double-wattled cassowary. *Journal of Thermal Biology* 19(6): 423-430.
- Pough, F.H., and McFarland, W.N., 1976. A physical basis for head-body temperature differences in reptiles. *Comparative Biochemistry and Physiology* 53A: 301-303.
- Ruben, J.A., 1995. Respiratory turbinates and the metabolic status of some theropod dinosaurs and *Archaeopteryx*. *Journal of Vertebrate Paleontology* 15(supplemental): 50A.
- Ruben, J.A., Dal Sasso, C., Geist, N.R., Hillenius, W.J., Jones, T.D., and Signore, M., 1999. Pulmonary function and metabolic physiology of theropod dinosaurs. *Science* 283: 514-516.
- Ruben, J.A., Hillenius, W.J., Geist, N.R., Leitch, A., Jones, T.D., Currie, P.J., Horner, J.R., and Espe, G., 1996. The metabolic status of some late Cretaceous dinosaurs. *Science* 273: 1204-1207.
- Ruxton, G.D., 2000. Statistical power analysis: application to an investigation of dinosaur thermal physiology. *Journal of the Zoological Society of London* 252: 239-241.
- Sellwood, B.W., Price, G.D., and Valdes, P.J., 1994. Cooler estimates of Cretaceous temperatures. *Nature* 370: 453-455.
- Seymour, R.S., and Lillywhite, H.B., 2000. Hearts, neck posture and metabolic intensity of sauropod dinosaurs. *Proceedings of the Royal Society of London B* 267: 1883-1887.
- Smith, E.N., 1979. Behavioral and physiological thermoregulation of crocodylians. *American Zoology* 19: 239-247.

- Spotila, J.R., Lommen, P.W., Bakkan, G.S., and Gates, D.M., 1973. A mathematical model for body temperatures of large reptiles: implications for dinosaur ecology. *The American Naturalist* 107(955): 391-404.
- Spotila, J.R., O'Connor, M.P., Dodson, P., and Paladino, F.V., 1991. Hot and cold running dinosaurs: body size, metabolism and migration. *Modern Geology* 16: 203-227.
- Spotila, J.R., Soule, O.H., and Gates, D.M., 1972. The biophysical ecology of the alligator: heat energy budgets and climate spaces. *Ecology* 53(6): 1094-1102.
- Stoskopf, M.K., Barrick, R.E., and Showers, W.J., 2001. Oxygen isotope variability in bones of wild caught and constant temperature reared sub-adult American alligators. *Journal of Thermal Biology* 26: 183-191.
- Stovall, J.W., and Langstrom, W., 1950. *Acrocantosaururus atokensis*, a new genus and species of lower Cretaceous Theropoda from Oklahoma. *The American Midland Naturalist* 43(3): 696-728.
- Taylor, C.R., 1972. The desert gazelle: a paradox resolved. *Symposia of the Zoological Society of London* 31: 215-227.
- Tracey, C.R., 1983. Biophysical modeling in reptilian physiology and ecology. In: Gans, C., and Pough, F.H., eds. *Biology of the Reptilia*, vol.12. Academic Press, London.
- Tracey, C.R., Turner, J.S., and Huey, R.B., 1986. A biophysical analysis of possible thermoregulatory adaptations in sailed pelycosaurs. In: Holton III, N., MacLean, P.D., Roth, J.D., and Roth, E.C., eds. *The Ecology and Biology of Mammal-like Reptiles*. Smithsonian Institution Press, Washington.
- Tudge, A.P., 1960. A method of analysis of oxygen isotopes of orthophosphates: its use in the measurement of paleotemperatures. *Geochimica et Cosmochimica Acta* 18: 81-93.
- Turner, J.S., and Tracey, C.R., 1983. Blood flow to appendages and the control of heat exchange in American alligators. *Physiological Zoology* 56(2): 195-200.
- Turner, J.S., and Tracey, C.R., 1986. Body size, homeothermy and the control of heat exchange in mammal-like reptiles. In: Holton III, N., MacLean, P.D., Roth, J.D., and Roth, E.C., eds. *The Ecology and Biology of Mammal-like Reptiles*. Smithsonian Institution Press, Washington.
- Urey, H.C., Lowenstam, H.A., Epstein, S., and McKinney, C.R., 1951. Measurement of paleotemperatures and temperatures of the Upper Cretaceous of England, Denmark, and the southeastern United States. *Bulletin of the Geological Society of America* 62: 399-416.
- Wilber, C.G., Robinson, P.F., and Hunn, J.B., 1961. Heart size and body size in fish. *Anatomical Record* 140(4): 285-287.
- Williams, T.M., 1990. Heat transfer in elephants: thermal partitioning based on skin temperature profiles. *Journal of the Zoological Society of London* 222: 235-245.

- Wilson, P.A., and Norris, R.D., 2001. Warm tropical ocean surface and global anoxia during the mid-Cretaceous period. *Nature* 412: 425-429.
- Winkler, D.A., Murry, P.A., Jacobs, L.L., 1989. Field guide to the vertebrate paleontology of the Trinity Group, Lower Cretaceous of Central Texas. Field Guide for the 49th Annual Meeting of the Society of Vertebrate Paleontology, Austin.
- Wright, P.G., 1984. Why do elephants flap their ears? *South African Journal of Zoology* 19(4): 266-269.

APPENDIX I – Data Tables

Alligator Data

*All temperature variation calculations are based on data from bone phosphates.
 ? indicates unknown bone type. These data were not used in calculations requiring specific identification of bone type.

Sample	Bone	Bone Type in Hole	Phosphate delta 18O (V-SMOW)	Carbonate delta 18O (V-SMOW)
NCSU#2-94				
410A	Femur	dense	18.20	
410B	Femur	dense	18.93	
410C	Femur	dense	19.24	
410D	Femur	dense	19.15	
410E	Femur	spongy	19.57	
410F	Femur	dense		27.721
410H	Femur	dense		25.508
410I	Femur	spongy		28.190
410J	Femur	dense		23.712
410K	Femur	spongy		28.706
410avg			19.02	27.449
range			1.37	4.993
411A	Tibia	dense	18.96	
411B	Tibia	dense	18.53	
411C	Tibia	dense	19.29	
411D	Tibia	dense	19.20	
411E	Tibia	spongy	19.98	
411avg			19.19	
range			1.45	
412A	Phalange	dense	19.02	
412B	Phalange	dense	19.18	
412C	Phalange	dense	18.85	
412D	Phalange	dense	19.51	
412E	Phalange	spongy	20.04	
412F	Phalange	dense		24.744
412G	Phalange	spongy		26.620
412H	Phalange	dense		24.737
412I	Phalange	dense		25.270
412J	Phalange	spongy		28.060
412avg			19.32	25.886
range			1.19	3.323

413A	Thoracic Vert (dorsal)	dense	19.54	
413B	Thoracic Vert (dorsal)	spongy	19.31	
413C	Thoracic Vert (dorsal)	spongy	20.04	
			19.39	
			19.29	
413D	Thoracic Vert (dorsal)	?	19.43	
413E	Thoracic Vert (dorsal)	?	19.53	
413avg			19.50	
range			0.75	
414A	Mid tail Vert	dense	19.28	
414B	Mid tail Vert	spongy	19.76	
414C	Mid tail Vert	spongy	19.60	
414D	Mid tail Vert	?	19.34	
414E	Mid tail Vert	dense	18.17	
414avg			19.23	
range			1.59	
461A	Tail Vert	dense		24.414
461B	Tail Vert	spongy		27.118
461C	Tail Vert	dense/spongy		25.170
461avg				25.567
range				2.704
415A	Distal tail Vert	?	18.98	
415B	Distal tail Vert	spongy	19.20	
415C	Distal tail Vert	?	19.30	
415D	Distal tail Vert	spongy	18.79	
415avg			19.07	
range			0.51	
416A	Humerus	dense	19.97	
416B	Humerus	dense	22.08	
416C	Humerus	dense	19.06	
			19.12	
416D	Humerus	dense	19.11	
416E	Humerus	spongy	19.97	
416F	Humerus	dense		24.780
416G	Humerus	spongy		26.290
416H	Humerus	dense		25.247
416J	Humerus	dense		25.037
416K	Humerus	spongy		29.016
416avg			19.89	26.872
range			3.02	4.236

417A	Lumbar Vert (dorsal)	dense	18.79	
417B	Lumbar Vert (dorsal)	spongy	19.61	
417C	Lumbar Vert (dorsal)	spongy	19.44	
			19.73	
417D	Lumbar Vert (dorsal)		16.94	
417E	Lumbar Vert (dorsal)		20.47	
460A	Dorsal Vert	dense		26.327
460B	Dorsal Vert	spongy		27.835
460C	Dorsal Vert	dense		
460D	Dorsal Vert	spongy		
460E	Dorsal Vert	dense/spongy		26.580
460F	Dorsal Vert	dense/spongy		25.595
dorsalavg			19.16	26.585
range			3.53	2.240
mid avg				27.081
NCSU-G7				
001A	Palatine	dense	18.6	25.400
001B	Palatine	spongy	17.5	24.389
001avg			18.1	24.894
range			1.1	1.010
002A	Maxilla	dense	19.7	28.869
002B	Maxilla	spongy	19.6	24.807
002avg			19.7	26.838
range			0.1	4.063
003A	Dentary	dense	17.2	24.799
003B	Dentary	dense	18.1	27.851
003C	Dentary	spongy		24.239
003avg			17.7	25.629
range			0.9	3.612
004A	Braincase	dense/spongy	18.8	25.408
004avg			18.8	25.408

Sample	Phosphate delta 18O (V-SMOW)	Carbonate delta 18O (V-SMOW)	Interbone Temperature Difference*	Temperature Difference from Core*	Intrabone Temperature Difference*
NCSU#2-94					
410avg	19.02	27.449	0.00	2.09	
range	1.37	4.993			5.89
411avg	19.19		0.75	1.34	
range	1.45				6.24
412avg	19.32	25.886	1.30	0.79	
range	1.19	3.323			5.12
413avg	19.50		2.09	0.00	
range	0.75				3.23
414avg	19.23		0.91	1.18	
range	1.59				6.84
415avg	19.07		0.21	1.88	
range	0.51				2.19
416avg	19.89	26.872	3.73	-1.64	
range	3.02	4.236			12.99
417avg	19.16		0.62	1.46	
range	3.53				15.18
NCSU-G7					
001avg	18.1	24.894	1.7		
range	1.1	1.010			4.7
002avg	19.7	26.838	8.6		
range	0.1	4.063			0.4
003avg	17.7	25.629	0.0		
range	0.9	3.612			3.9
004avg	18.8	25.408	4.9		

Elephant Data

*All temperature variation calculations are based on data from bone phosphates.

Sample	Bone	Bone Type in Hole	Phosphate delta 18O (V-SMOW)	Carbonate delta 18O (V-SMOW)
002A	Lumber Vert #24	dense	17.2	25.796
002B	Lumber Vert #24	spongy	17.3	25.202
002C	Lumber Vert #24	spongy	17.2	25.038
002D	Lumber Vert #24	dense	17.0	23.735
002E	Lumber Vert #24	dense	16.5	31.041
002avg			17.2	24.943
range			0.3	2.062
003A	Caudal Vert #12	dense		25.175
003B	Caudal Vert #12	dense	18.0	29.301
003C	Caudal Vert #12	spongy	18.3	28.226
003D	Caudal Vert #12	spongy	17.9	28.535
003E	Caudal Vert #12	spongy	17.9	22.928
003avg			18.0	26.833
range			0.4	6.374
005A	Rib #10 (proximal)	dense	16.4	27.760
005B	Rib #10 (proximal)	dense	16.7	26.416
005C	Rib #10 (proximal)	dense	16.6	26.461
005D	Rib #10 (proximal)	spongy	16.8	22.315
005E	Rib #10 (proximal)	spongy	16.9	24.293
005proxavg			16.7	25.449
range			0.5	5.445
005F	Rib #10 (distal)	dense	16.2	24.382
005G	Rib #10 (distal)	dense	17.1	25.900
005H	Rib #10 (distal)	dense	16.5	25.115
005I	Rib #10 (distal)	spongy	16.7	25.887
005distalavg			16.6	25.321
range			0.9	1.517

007A	Femur	dense	17.8	24.836
007B	Femur	dense	16.3	25.442
007C	Femur	dense	16.8	25.741
007D	Femur	dense	16.8	28.615
007E	Femur	spongy	17.2	25.690
007avg			17.0	26.065
range			1.5	3.779
009A	Tibia	dense	17.1	27.969
009B	Tibia	dense	17.3	24.309
009C	Tibia	dense	16.7	25.534
009D	Tibia	spongy	16.6	27.563
009E	Tibia	spongy	16.6	25.122
009avg			16.9	26.099
range			0.7	3.661
011A	Metatarsal II	dense	17.0	22.239
011B	Metatarsal II	spongy	16.8	23.265
011C	Metatarsal II	spongy	16.9	20.374
011D	Metatarsal II	spongy	17.0	24.060
011E	Metatarsal II	spongy	16.9	24.071
011avg			16.9	22.802
range			0.2	3.697

Sample	Phosphate delta 18O (V-SMOW)	Carbonate delta 18O (V-SMOW)	Interbone Temperature Difference*	Temperature Difference from Core*	Intrabone Temperature Difference*
002avg	17.2	24.943	2.4	0.0	
range	0.3	2.062			1.3
003avg	18.0	26.833	6.0	-3.7	
range	0.4	6.374			1.7
005proxavg	16.7	25.449	0.2	2.1	
range	0.5	5.445			2.2
005distalavg	16.6	25.321	0.0	2.4	
range	0.9	1.517			3.9
007avg	17.0	26.065	1.5	0.8	
range	1.5	3.779			6.5
009avg	16.9	26.099	1.0	1.4	
range	0.7	3.661			3.0
011avg	16.9	22.802	1.3	1.1	
range	0.2	3.697			0.9

Ostrich Data

*All temperature variation calculations are based on data from bone phosphates.

Sample	Bone	Bone Type in Hole	Phosphate delta 18O (V-SMOW)	Carbonate delta 18O (V-SMOW)
102A	Tibia	dense	16.6	25.675
102B	Tibia	dense	15.9	24.508
102D	Tibia	dense	15.2	23.514
102E	Tibia	dense	14.7	24.466
102avg			15.6	25.804
range			1.9	2.161
104A	Femur	dense	15.3	24.622
104B	Femur	dense	16.7	24.748
104C	Femur	dense	16.3	23.957
104D	Femur	dense	15.4	23.660
104E	Femur	dense	14.9	22.304
104avg			15.7	23.858
range			1.8	2.444
105A	Metatarsal	dense	15.6	23.592
105B	Metatarsal	dense	15.5	23.606
105C	Metatarsal	dense	14.8	25.388
105D	Metatarsal	dense	15.4	25.474
105E	Metatarsal	dense	15.3	23.942
105avg			15.3	24.400
range			0.8	1.881
107A	Ulna	dense	15.6	24.247
107B	Ulna	dense	15.5	22.813
107C	Ulna	dense	15.3	23.690
107D	Ulna	dense	15.1	23.257
107E	Ulna	spongy	15.6	26.156
107avg			15.4	24.033
range			0.5	3.343
112A	Dorsal Vert (centrum)	dense	15.1	23.206
112B	Dorsal Vert (centrum)	spongy	15.4	22.298
112avg			15.3	22.752
range			0.3	0.908
113B	Dorsal Vert (spine)	spongy	15.4	23.924
113avg			15.4	24.069
range				0.289

112&113avg			15.3	
range			0.3	
114A	Cervical Vert (centrum)	dense	15.6	22.320
114B	Cervical Vert (centrum)	spongy	15.0	26.841
114avg			15.3	24.581
range			0.6	4.520
115A	Cervical Vert (spine)	dense	15.4	23.803
115B	Cervical Vert (spine)	spongy	15.5	24.291
115avg			15.5	24.047
range			0.1	0.489
114&115avg			15.4	
range			0.6	
117A	Phalange	dense	14.8	23.005
117B	Phalange	dense	15.0	25.707
117C	Phalange	dense	14.5	22.330
117D	Phalange	spongy		22.445
117avg			14.8	23.372
range			0.5	3.377
118A	Palatine	dense	15.8	22.988
118B	Palatine	spongy	16.1	22.799
118avg			16.0	22.894
range			0.3	0.095
119A	Palatine (anterior)/Vomer	dense	15.5	26.103
119B	Palatine (anterior)/Vomer	spongy	15.8	22.151
119avg			15.7	24.127
range			0.3	3.951
120A	Dentary	dense	16.2	29.329
120B	Dentary	spongy		22.952
120avg			16.2	26.141
range				6.377
121A	Braincase	dense		24.738
121B	Braincase	spongy		22.450
121avg				23.594
range				2.287

Sample	Phosphate delta 18O (V-SMOW)	Carbonate delta 18O (V-SMOW)	Interbone Temperature Difference*	Temperature Difference from Core*	Intrabone Temperature Difference*
102avg	15.6	25.804	3.6	-1.3	
range	1.9	2.161			8.2
104avg	15.7	23.858	4.1	-1.8	
range	1.8	2.444			7.7
105avg	15.3	24.400	2.4	-0.1	
range	0.8	1.881			3.4
107avg	15.4	24.033	2.8	-0.5	
range	0.5	3.343			2.2
112&113avg	15.3		2.3	0.0	
range	0.3				1.3
114&115avg	15.4		2.6	-0.3	
range	0.6				2.6
117avg	14.8	23.372	0.0	2.3	
range	0.5	3.377			2.2
118avg	16.0	22.894	5.1	-2.8	
range	0.3	0.095			1.3
119avg	15.7	24.127	3.8	-1.5	
range	0.3	3.951			1.3
120avg	16.2	26.141	6.1	-3.9	
range		6.377			0.0

***Acrocanthosaurus atokensis* Data**

*All temperature variation calculations are based on data from bone phosphates.

Sample	Bone	Bone Type in Hole	Phosphate delta 18O (V-SMOW)	Structural Carbonate delta18O (V-SMOW)	Cement Carbonate delta18O (V-SMOW)
102A	Gastralia (proximal)	dense	20.5	28.378	
102B	Gastralia (proximal)	spongy	21.5	28.891	
102C	Gastralia (proximal)	spongy	21.6	29.032	
102proxavg			21.2	28.767	
range			1.1	0.655	
102F	Gastralia (distal)	dense	21.7	28.506	
102G	Gastralia (distal)	dense	22.2	28.236	
102distavg			22.0	28.371	
range			0.5	0.269	
103A	Ulna	dense	22.4	30.037	31.451
103B	Ulna	dense		30.056	
103C	Ulna	dense/spongy		29.851	
103E	Ulna	spongy		30.178	
103F	Ulna	spongy	20.6	30.502	
103avg			21.5	30.247	
range			1.8	0.652	
107A	Sacral Spine (distal)	dense	20.8	29.397	29.629
107B	Sacral Spine (distal)	dense	20.6	30.360	30.121
107C	Sacral Spine (distal)	dense	20.5	29.828	29.329
107D	Sacral Spine (distal)	spongy	20.8	29.336	28.760
107disavg			20.7	29.730	
range			0.3	1.024	
107E	Sacral Spine (mid)	dense	21.1	30.538	29.402
107F	Sacral Spine (mid)	dense	21.4	30.303	29.831
107G	Sacral Spine (mid)	spongy	21.3	29.873	29.246
107H	Sacral Spine (mid)	spongy	20.7	29.421	28.695
107midavg			21.1	30.034	
range			0.7	1.117	

107I	Sacral Spine (proximal)	dense	21.0	30.336	26.225
107J	Sacral Spine (proximal)	dense	20.6	30.363	28.221
107K	Sacral Spine (proximal)	spongy	20.4	28.968	28.319
107L	Sacral Spine (proximal)	spongy	20.7	29.419	30.703
107proxavg			20.7	29.772	
range			0.6	1.395	
108A	Pterygoid	dense	20.2	30.909	
108B	Pterygoid	dense	20.7	31.049	
108C	Pterygoid	spongy	21.2	30.477	
108D	Pterygoid	spongy	20.7	27.563	
108avg			20.7	29.999	
range			1.0	3.485	
109A	Palatal	dense	21.6	29.833	32.062
109B	Palatal	dense	21.3	29.702	29.208
109C	Palatal	spongy	21.5	29.727	31.138
109D	Palatal	spongy	21.3	29.928	30.759
109avg			21.4	29.798	
range			0.3	0.226	
110A	Vomer	dense	21.2	29.575	
110B	Vomer	spongy		30.351	
110avg			21.2	29.963	
range				0.776	
111A	Caudal #25 (centrum)	dense	22.0	29.071	
111B	Caudal #25 (centrum)	spongy	22.4	29.228	
111C	Caudal #25 (centrum)	spongy	21.6	28.810	
111D	Caudal #25 (centrum)	spongy	21.6	28.961	
111avg			21.9	29.018	
range			0.8	0.419	
112A	Chevron (caudal #26)	spongy	20.6	28.255	
112avg					

113A	Dorsal Rib (proximal)	dense	22.1	29.785	
113B	Dorsal Rib (proximal)	dense	20.5	28.904	
113C	Dorsal Rib (proximal)	dense	20.9	29.214	
113D	Dorsal Rib (proximal)	dense	21.3	29.334	
113E	Dorsal Rib (proximal)	spongy	21.1	28.190	
113proxavg			21.2	29.085	
range			1.6	1.595	
113F	Dorsal Rib (distal)	dense	21.3	30.029	
113G	Dorsal Rib (distal)	dense	21.2	29.504	
113H	Dorsal Rib (distal)	dense	22.1	29.203	
113I	Dorsal Rib (distal)	spongy	21.9	29.724	
113J	Dorsal Rib (distal)	spongy	20.7	29.315	
113disavg			21.4	29.555	
range			1.4	0.826	
114A	Dentary	dense	20.9	29.377	
114B	Dentary	dense	20.4	31.831	
114C	Dentary	dense	20.4		
114D	Dentary	spongy	19.6	32.229	
114E	Dentary	spongy	19.9	30.866	
114avg			20.2	31.076	
range			1.2	2.852	
115A	Braincase	dense	19.4	30.324	
115B	Braincase	dense	19.1	30.233	29.803
115C	Braincase	spongy	19.5	30.340	29.274
115D	Braincase	spongy	19.4	29.355	29.504
115avg			19.3	30.063	
range			0.5	0.986	
116A	Tibia	dense	21.3	31.553	
116B	Tibia	dense	20.6	30.980	
116C	Tibia	dense	21.1	29.618	
116E	Tibia	dense		30.814	
116F	Tibia	spongy	21.3	30.857	
116avg			21.1	30.764	
range			0.8	1.935	
117A	Femur	dense	21.2	30.052	
117B	Femur	dense	19.9	29.417	
117C	Femur	dense	21.1	30.104	
117D	Femur	dense	21.7	30.137	
117E	Femur	spongy	21.0	30.225	
117midavg			21.0	29.987	
range			1.8	0.808	

120A	Metatarsal	dense	21.3		
120B	Metatarsal	dense	20.5		
120C	Metatarsal	spongy	21.3		
120D	Metatarsal	spongy	20.1		
120E	Metatarsal	spongy	20.2		
120avg			20.7		
range			1.2		

Sample	Phosphate delta 18O (V-SMOW)	Structural Carbonate delta18O (V-SMOW)	Interbone Temperature Difference*	Temperature Difference from Core*	Intrabone Temperature Difference*
102proxavg	21.2	28.767	8.0	-0.1	
range	1.1	0.655			4.7
102distavg	22.0	28.371	11.3	-3.4	
range	0.5	0.269			2.2
103avg	21.5	30.247	9.3	-1.4	
range	1.8	0.652			7.7
107disavg	20.7	29.730	5.7	2.2	
range	0.3	1.024			1.1
107midavg	21.1	30.034	7.7	0.2	
range	0.7	1.117			3.0
107proxavg	20.7	29.772	5.7	2.2	
range	0.6	1.395			2.5
108avg	20.7	29.999	5.9	2.0	
range	1.0	3.485			4.3
109avg	21.4	29.798	9.0	-1.1	
range	0.3	0.226			1.5
110avg	21.2	29.963	8.0	-0.1	
range		0.776			0.0
111avg	21.9	29.018	11.1	-3.1	
range	0.8	0.419			3.4
113proxavg	21.2	29.085	7.9	0.0	
range	1.6	1.595			6.7
113disavg	21.4	29.555	9.1	-1.2	
range	1.4	0.826			6.0
114avg	20.2	31.076	3.9	4.0	
range	1.2	2.852			5.3
115avg	19.3	30.063	0.0	7.9	
range	0.5	0.986			2.0

116avg	21.1	30.764	7.4	0.5	
range	0.8	1.935			3.2
117midavg	21.0	29.987	7.1	0.9	
range	1.8	0.808			7.7
120avg	20.7		5.8	2.1	
range	1.2				5.2